

Thermal Spray Processes in Concentrating Solar Power Technology

Felice Rubino ^{1,*}, Pedro Poza ¹, Germana Pasquino ² and Pierpaolo Carlone ³ 

¹ Department of Chemical, Energetic and Mechanical Technology, University Rey Juan Carlos, Campus of Móstoles, Calle Tulipán s/n, 28933 Móstoles, Spain; pedro.poz@urjc.es

² Universitas Mercatorum, Piazza Mattei, 10, 00186 Rome, Italy; germana.pasquino@unimercatorum.it

³ Department of Industrial Engineering, University of Salerno, Via Giovanni Paolo II, 132, 84084 Fisciano, Italy; pcarlone@unisa.it

* Correspondence: felice.rubino@urjc.es; Tel.: +34-96-488-8142

Abstract: Solar power is a sustainable and affordable source of energy, and has gained interest from academies, companies, and government institutions as a potential and efficient alternative for next-generation energy production. To promote the penetration of solar power in the energy market, solar-generated electricity needs to be cost-competitive with fossil fuels and other renewables. Development of new materials for solar absorbers able to collect a higher fraction of solar radiation and work at higher temperatures, together with improved design of thermal energy storage systems and components, have been addressed as strategies for increasing the efficiency of solar power plants, offering dispatchable energy and adapting the electricity production to the curve demand. Manufacturing of concentrating solar power components greatly affects their performance and durability and, thus, the global efficiency of solar power plants. The development of viable, sustainable, and efficient manufacturing procedures and processes became key aspects within the breakthrough strategies of solar power technologies. This paper provides an outlook on the application of thermal spray processes to produce selective solar absorbing coatings in solar tower receivers and high-temperature protective barriers as strategies to mitigate the corrosion of concentrating solar power and thermal energy storage components when exposed to aggressive media during service life.

Keywords: clean energy; concentrating solar power; selective solar absorber; sustainable manufacturing technologies; thermal energy storage; thermal spray processes



Citation: Rubino, F.; Poza, P.; Pasquino, G.; Carlone, P. Thermal Spray Processes in Concentrating Solar Power Technology. *Metals* **2021**, *11*, 1377. <https://doi.org/10.3390/met11091377>

Academic Editor: Robert B. Heimann

Received: 11 June 2021

Accepted: 27 August 2021

Published: 31 August 2021

Publisher's Note: MDPI stays neutral with regard to jurisdictional claims in published maps and institutional affiliations.



Copyright: © 2021 by the authors. Licensee MDPI, Basel, Switzerland. This article is an open access article distributed under the terms and conditions of the Creative Commons Attribution (CC BY) license (<https://creativecommons.org/licenses/by/4.0/>).

1. Introduction

After photovoltaic (PV), concentrated solar power (CSP) is the second class of solar technology adopted worldwide to exploit solar energy to produce electricity. CSP plants use mirrors to reflect and focus solar radiation to heat a thermal fluid [1], which can be gas, solid particles or fluid steam [2], oil, or molten salts [3–5]), that is used to drive turbines in a power cycle and generate electricity [6,7] (see Figure 1). The thermal fluid can be directly integrated into the power cycle and expand in the turbines, or used to transfer the accumulated heat to a separate fluid [6,7]. Depending on the technical solution adopted for the plant, solar radiation is reflected by mirrors and focused on a pipe (in the case of a parabolic design, as shown in Figure 1, or linear Fresnel reflector) through which flows the heated fluid or directed to a single central receiver (the central solar power tower design or the parabolic dish system) [8]. Compared to the photovoltaic (PV) system, CSP technology can only be used on a large scale to make energy production economic, due to their high capital costs, and does not have PV's modularity. CSP comes, however, with very intriguing benefits. First, in contrast to PV technology, CSP can incorporate an energy storage system, which allows for the production of electricity even during night hours or with no sunlight. Second, being similar to a conventional thermal power plant, CSP can be coupled with fossil fuel generators to build hybrid plants, in particular with natural gas power systems [6,9,10].

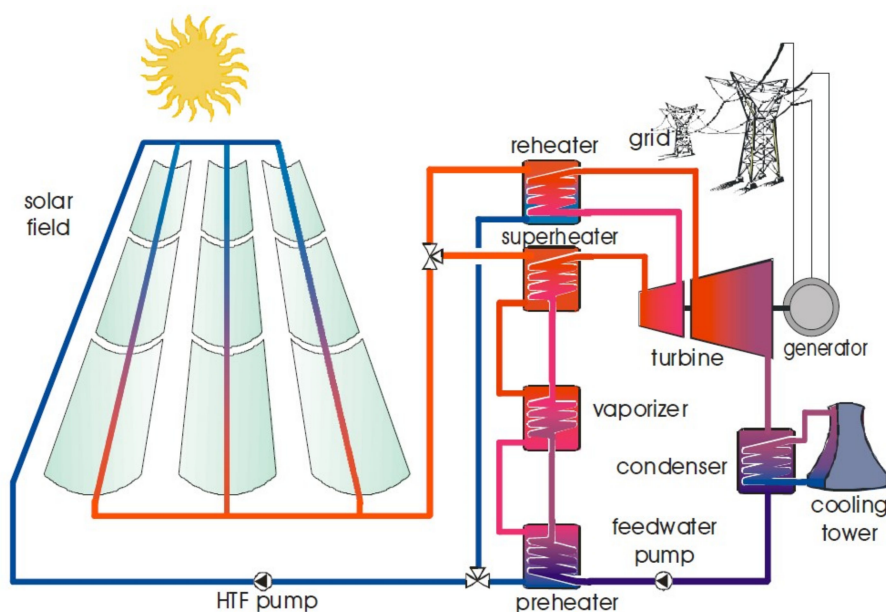


Figure 1. Scheme of the working principle of a CSP plant equipped with parabolic trough collector receiver and connected to a power cycle system, adapted from [11].

In turn, however, it suffers from the same thermodynamic limitations and its heat–electricity conversion efficiency depends on the working temperatures. Until now, indeed, the heat collected from the sun is not at the same level as the fossil-fuel plants, therefore the efficiency of CSP plants is lower than that of the conventional thermal plants. Figure 2 below depicts the energy flow and the losses in a CSP plant [12], from the solar radiation collected by the receiver to the delivery of electricity in the grid. By observing the images, note that less than half of the total incident energy, approximately 40%, is transferred to the thermal fluid operating in the power cycle, which results from energy losses due to the CSP systems associated with the mirrors and the receiver. After that, further reduction is due to the thermodynamic of the power cycle, usually Rankine, Brighton, or Sterling cycles; therefore only 40% of the gathered heat is converted into electricity, which depends on the lower temperatures achievable within the concentrating solar system. It reduces the global efficiency of the plant to 16% of the total energy available from solar radiation. In that scenario, increasing the operating temperature of heat thermal fluid (HTF) circulating within the receiver (above 600 °C) and, therefore, the temperatures of the power cycles could be beneficial to the efficiency of the heat-to-electricity conversion [13].

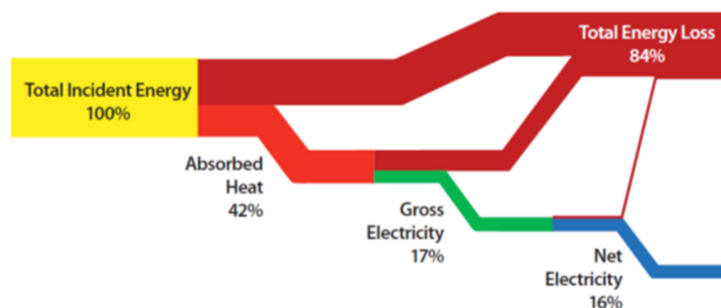


Figure 2. The efficiency of a typical CSP plant [12].

By analyzing the energy flows depicted in Figure 2, it can be argued that the main losses are attributed to the capability of the CSP system to collect the energy brought by the solar radiation; meanwhile, the efficiency of the turbines in CSP plants and conventional thermal plants are comparable. It suggests that losses in solar-to-heat conversion can be reduced by improving the mirror system and the central receivers. Research in novel

designs of the CSP system components and advanced materials can lead to significant improvements in the efficiency of solar plants. In the last few decades, indeed, CSP technologies have been the subject of intensive studies and research activities aiming to improve the efficiency of the plants and make solar-generated electricity more cost-effective, as demonstrated by patent documents published in the very recent years [14]. While these efforts were directed mainly toward different aspects of the CSP, the improvement in the exploitation of energy from solar radiation and in dispatchability of electricity produced by CSP plants have encountered particular attention [14]. In the former case, one of the goals was to increase the amount of energy that can be collected from the sun's rays by the receivers, which concurs to almost 50% of the energy losses in CSP plants [11]. In the latter case, the strategies proposed by designers involved the adoption of a working fluid operating at higher temperatures to increase the efficiency of the energy storage systems and the use of high-performance materials to increase the durability and lifetime of the system components.

Thermal spraying (TS) has encountered a growing interest by researchers and companies active in the solar energy field, which explored the integration of TS technologies in the production of solar absorber coatings and corrosion barriers within the components of CSP and thermal energy storage (TES) systems, as an efficient and cost-effective alternative to currently employed methodologies. The purpose of this work is to gather the contributions from published literature and provide an overview on the state of the art concerning the application of thermal spray technologies within the CSP technologies. Emphasis is on solar power systems, which can particularly benefit from the properties of thermal sprayed coatings. Research organizations and companies directly involved in the development of the CSP systems together with experts working in the surface modification sector can be a potential audience of the present work, allowing them to explore novel solutions and identify new markets in their respective fields of interest. The remainder of the paper is organized as follows: Section 2 describes the literature on the solar selective absorber and the application of thermal spray process to manufacture absorbent coatings. Section 3 reviews the literature on the corrosion mitigation strategies adopted by designers and producers, with emphasis on the protective barrier manufactured by thermal spraying.

2. Thermal Spray Processes for Manufacturing Solar Selective Coatings

2.1. Introduction

As described previously, concentrating solar power technologies rely on reflectors (or mirrors) to collect the solar radiation and focus it at a certain level of concentration onto a line- or point-receiver, also called the absorber, which converts the sun's rays to heat. Therefore, the working principles of the active components in a CSP system are based on the reflection, absorbance, and transmittance of light. These phenomena are influenced by many factors: the physical state of the materials (gas, solid, or liquid), physical and chemical properties, surface features and texture, light wavelength, and incidence angle.

The efficiency of receivers in a CSP plant depends on the amount of energy they can absorb from solar radiation. Maximizing the absorption of solar energy and reducing the heat losses from the receiver to the environment (i.e., the thermal emittance) are the key factors to increase the solar-to-heat efficiency, which constitutes almost 40% of the energy balance in a CSP plant (Figure 2) [12]. It means that receivers should have optimized optical properties and microstructure stability in the operative temperature range. In particular, the selective absorbers must be characterized by high absorptivity in the solar spectrum (i.e., wavelength of 250–2500 nm), to maximize the solar energy captured, and low emissivity (also referred to as thermal emittance, ε) in the infrared spectrum (i.e., wavelength of 1.5–2.5 μm) at the operative temperatures to minimize the heat losses. Values of absorptance (α) above 0.95 and ε less than 0.05 are highly desirable but challenging to attain. The structural materials, e.g., steels and aluminum alloys, usually employed in the construction of the elements that compose the CSP plants (namely heliostats, collectors, and receivers) do not provide the required optical properties necessary for efficient exploitation of solar energy.

For this reason, coatings are used to cover the surface of these elements to achieve the optimal values of solar absorptance, reflectance, and thermal emittance, and simultaneously improving (when possible) the structural integrity of CSP components. In addition, coating materials must be stable in the air under cyclic loads, have a low-cost, and a large scalability to improve the overall efficiency of the CSP plant. In PTC systems, the absorbing coatings are already optimized, and they operate in a vacuum and with very protective conditions. In contrast, receivers in CPT systems usually operate in the air, therefore severe issues come from the exposure to reactive environments and the action of erosion, pollution, etc. These factors make the design of proper absorbing coatings for the receiver in the solar towers more challenging.

Currently, the standard for coating in the central receiver of CPT plants is the Pyromark 2500 paint. It provides a remarkable value of the absorptance from 0.96 at near-normal incidence to approximately 0.8 at glancing incident angle. However, Pyromark is characterized by a high thermal emittance that ranges from 0.8 at 100 °C up to 0.9 at 1000 °C and, thus, suffers from significant thermal losses [15,16]. In addition, Pyromark 2500 paint degrades rapidly if operated in air at high temperature. Ho et al. [16] observed a reduction of several percentage points after 300 h if exposed at the operating temperature of 750 °C. Therefore, Pyromark coating requires frequent maintenance (annual or biannual) to maintain the performance, determining relatively high operational costs (i.e., maintenance and shutdown costs) of the CSP plants. To promote the competitiveness of CSP in the electricity market, new durable absorber materials able to withstand operating temperatures above 650 °C and heating/cooling cycles, cost-effective, and easy to be applied are needed. At the same time, materials need to be conceived to have the lowest radiative and convective losses that reduce the thermal efficiency of the receivers, to retain their structural integrity after thousands of thermal cycles, and to protect the structural component from external factors (erosion, action of wind, dust, hail, etc.). Ceramics, metals, and combinations of both are currently employed as solar selective coatings [17–19].

To be used in CSP applications, the materials should be thermally stable at temperatures above 400 °C and retain their optical properties. Several materials and coating structures have been developed in the past few decades, aiming to obtain solar absorbers with higher optical properties and higher thermal stability. According to the most recent studies [20], three classes of high-temperature coating have been identified depending on the type of the absorbing dielectric: double cermet solar selective coatings, transition metal nitride multilayer coatings, and transition metal oxide multilayer coatings. However, many materials fall within these classes, and describing their advantages and disadvantages is beyond the scope of the present review. The readers may read the works of Kennedy [18], Atkinson [19], and Xu [20] for more exhaustive information about the materials used and their chemical composition, the typical configurations of the coatings, the field of application, and the main failure mechanisms.

2.2. Thermal Spray Processes for Selective Absorber

Besides the materials and the structure of the coating, the selective optical properties have a direct correlation with the manufacturing techniques. Vacuum technologies, such as physical vapor deposition (PVD) or chemical vapor deposition (CVD), and wet chemical processing are the methods commonly adopted to develop selective solar coatings [19,21]. These processes have been mainly applied in PTC, where coatings are required to have a thickness in the order of microns. In CPT, where thicker coatings are necessary, these methods are not suitable. Wet chemical processes include painting and sol-gel processing and represent the lowest-cost techniques to produce absorber coating. As mentioned before, the absorber used most in solar tower applications is the Pyromark black paint. Indeed, it is easy to apply on central receivers and provides the greatest absorptance even at high temperature, despite it suffers thermal losses due to high thermal emittance [22]. In addition, several concerns arise regarding the mechanical integrity of these coatings, adhesion on the substrates, and their stability under thousands of heating/cooling cycles.

Vacuum processes are the consolidated technologies to manufacture absorber coatings that have high selectivity in their optical properties. PVD and CVD processes can produce films starting from a wide variety of metals, ceramics, and compounds; they also guarantee high reproducibility of the manufactured film owing to the accurate control in the process parameters [23]. However, they are characterized by high operating cost and small-scale production, and therefore not suitable for larger plants. Additionally, the optical properties of manufactured coatings degrade faster when exposed to high temperature and the atmosphere. For these reasons, vacuum processes are convenient in PTC systems, where the absorbers work in vacuum conditions but are not suitable for central tower systems. The development of stable and durable selective absorber coatings with tailored optical properties, production methods, and technologies for large-scale in situ applications is of paramount relevance to achieve high efficiency in central tower plants [24,25]. Thermal spray technologies allow application of ceramic and metal coatings on a wide variety of shapes and sizes of substrates, representing promising alternatives to the paint coatings and vacuum deposition technologies for the solar absorber. Indeed, thermal spraying is suitable for large-scale production and allows for deposition of coatings that range from a micron to a few millimeters in thickness. The main advantages of thermal spray processes can be summarized: (i) high stability, (ii) high production efficiency, (iii) low production costs, and (iv) simple operation. Those aspects make these technologies promising for solar applications [26]. However, thermal sprayed coatings come with poorer selective absorption properties when compared to vacuum-deposited absorbers due to microstructure flaws, surface roughness, and other reasons that are not yet been fully understood.

The main difference of thermal spraying coatings with respect to those produced with vacuum technologies is related to the heterogeneity of the material deposited. Thermal sprayed coatings are characterized by a complex microstructure and by open/closed porosities. Furthermore, they present a higher surface roughness. Several studies have pointed out the influence of porosities, grain boundaries, internal phases, and roughness on the optical properties of the coating [27,28]. Therefore, coatings produced by thermal spray technologies have different optical behavior compared to those deposited with the vacuum process.

The first attempt to use thermal spray processes to achieve tailored optical properties was made by Tului et al. [29], who deposited ZnO and Al₂O₃ mixed powders using controlled atmospheric plasma spray (CAPS). In their work, the authors analyzed the emissivity of the coatings in the visible and near-infrared (NIR) range and tried to establish a correlation between the amount of alumina content in the initial powder mixture with the optical behavior of the coatings. Devoted literature indicated the doping effect of the Al atoms inside the lattice structure of ZnO [30,31] that leads to a reduction of emissivity in the infrared region, even in low percentages (approximately 3% by weight). Using alumina instead of pure aluminum particles, the authors observed a decrease in the emissivity with the increase in the % of Al₂O₃ (from 3% to the eutectic 22% in weight). Process environment, i.e., air or protective inert gas (or IPS) atmosphere, also influenced the interaction with the sunlight. Spraying in an inert atmosphere reduced the rate of oxidation and led to the depletion of oxygen and, then, the formation of oxygen vacancies in the ZnO lattice structure, which acted as additional doping [32] and lowered the emissivity in the visible–NIR region. From the study of Tului et al. [29] emerged that the plasma spray can be potentially used in solar applications at least for the material system analyzed. However, emissivity remains high, especially in the middle infrared range, to be competitive. Therefore, more investigations are required, in particular regarding the optimization of the process itself and the thermal stability of the absorber coatings. However, no other published data about plasma spray and ZnO-based coating have been found in the literature.

After this preliminary study, researchers from the Sandia National Laboratories conducted a thorough analysis on several materials, metals, and ceramics, or their combination, which were already used in solar applications, by using thermal spray technology [24,25,33,34]. Ni-25 wt% Graphite, Ni-5Al, pure W, WC-20Co, WC-9Co, WC-25Ni,

CeO₂, Co-28Mo-17.5Cr-3.5Si, Co-28Mo-17.5Cr-3.5Si metals, and cermet systems were deposited using the APS process on steels and Ni-alloys substrates. Considering that the ideal selective optical properties, i.e., $\alpha > 0.95$ in the visible range and $\varepsilon < 0.3$ in IR region, are hardly achievable simultaneously in the deposited absorbers, the authors proposed a summarizing index called “factor of merit” (FOM) to aid in comparing the thermally sprayed coatings with the benchmark system [33]. The FOM is defined as:

$$\text{FOM}(\text{W}/\text{cm}^2) = 60 \cdot \alpha_{\text{solar}} - 5 \left[\frac{\varepsilon_{80^\circ\text{C}} + \varepsilon_{2400\text{nm}}}{2} \right] \quad (1)$$

where α_{solar} , $\varepsilon_{80^\circ\text{C}}$ and $\varepsilon_{2400\text{nm}}$ are the solar absorptance, emittance at 80 °C, and emittance at 2400 nm, respectively. The constants 60 and 5, having the units of W/cm², represent the energy flux incident on the receiver and the energy flux emitted at 700 °C in an environment at 20 °C. The index suggests that to improve the efficiency of the central receiver, maximizing the absorptance is more effective than minimizing the thermal emittance. Additionally, SPT receiver materials are opaque to solar energy; therefore, maximizing the receiver absorptance minimizes the reflectance from the receiver surface. The Pyromark 2500 paint, used as the benchmark, has a FOM of 53.3. The concept behind the application of APS to produce absorber coatings was to accept systems that can have lower FOM but are more durable and stable in high operating temperatures. To this scope, the authors also evaluated the thermal stability of the coating at different temperatures. The as-sprayed coatings did not perform well; the coatings had absorptance between 0.73 and 0.85 for WC-9Co and CeO₂, respectively, and thermal emittance between 0.3 (pure tungsten) and 0.62 (Ni-graphite cermet), achieving FOM in 35–48 range. Some materials have acceptable emittance; however, they also have an absorptance that is too low and then are not suitable for the receivers in as-sprayed form. Reducing the surface roughness, which is usually quite high after the plasma spray deposition, further lowered both optical properties. When the dimension of surface roughness is shorter than the wavelength of the solar rays, the surface is just the same as a mirror for these rays, and most of the infrared light is reflected from the surface; therefore, a lower ε also could be achieved [35]. In contrast, when the surface roughness is larger than the wavelength of sunlight, the electromagnetic wave is trapped by multiple reflections, contributing to better absorption properties. Smoother surfaces led to a decrease of FOM of the coating by 40%, dropping to as little as 7% [25,33].

Heat treatment at 600 °C led to an increase in absorptance and emittance of all coatings up to 0.95/0.78 (α/ε) in the case of Ni/graphite cermet and 0.89/0.49 for CeO₂ oxide, which performed the best with respect to the other systems. The heating of coating produced two distinct phenomena on the surface. From one side, it promotes the formation of an oxide and, if it is stable, an increase in the coating thickness; conversely, a reduction in roughness has been observed after the heat treatment. According to that, after the treatment, almost all coatings, regardless of the substrate, experience an increase in the FOM. The authors argued that changes in the oxide layer on top of the coating have a more relevant effect on the optical performance than the roughness, which conversely negatively influences light absorption. Ni-5Al metallic coating also proved to be a suitable candidate, achieving after the treatment optical properties competitive with the Pyromark 2500 (α/ε equal to 0.89/0.57) with a FOM of 50. Observed behavior has been linked to the formation of NiO and Al_xO_y oxides within the coating and the beneficial doping from Al particles. Pure tungsten and WC-Co coatings performed worse than other materials. Indeed, tungsten underwent pronounced oxidation with the WO_x oxide layer that resulted in poor adhesion on the substrate. Spalling phenomenon has been observed in the W-based coatings; the oxide scale together with fractures delaminates due to the different thermal coefficients with the underlying layers and the residual stresses arising from the treatment [24,25,34].

From this preliminary research, it emerged that thermal spray processes can be a suitable alternative to the vacuum deposition processes or dip-coating method, and the deposited materials are potentially competitive with the Pyromark 2500. However, besides the optical properties, other important features, such as adhesion, corrosion resistance to the

environment, and fatigue strength against thermal cyclic loads, have not been investigated; therefore, the long-term stability of these coatings has not been fully demonstrated. Table 1 summarizes the optical properties of the material system.

Table 1. Absorptance and emittance data for coatings with as-sprayed, with 1 μ polished, and with as-sprayed heat-treated surfaces (data from [24,25,33]).

Coating		α			ε_{80}			FOM (W/cm ²)	
Material	As Sprayed	Smooth Surface (Ra = 1 μ m)	Heat Treat.	As Sprayed	Smooth Surface (Ra = 1 μ m)	Heat Treat.	As Sprayed	Smooth Surface (Ra = 1 μ m)	Heat Treat.
Ni-25 Graphite	0.81	0.52	0.93	0.62	0.33	0.78	45	26	52
Ni-5Al	0.63	0.26	0.89	0.39	0.11	0.57	35	12	50
Tungsten	0.69	0.46	0.74	0.29	0.13	0.82	39	28	40
WC-20Co	0.82	0.60		0.55	0.32		46	37	
WC-9Co	0.73	0.45		0.53	0.24		40	28	
WC-25Ni	0.75	0.60		0.51	0.24		39	35	
CeO ₂	0.85	0.16	0.89	0.41	0.11	0.49	48	7	50
Co-28Mo-17.5Cr-3.5Si	0.79		0.86	0.48		0.61	44		48
Co-28Mo-17.5Cr-3.5Si	0.79		0.86	0.47		0.57	44		48

Sandia researchers investigated thermally sprayed absorbers at higher temperatures to assess their thermal stability in harsh conditions [34]. Lanthanum strontium manganate (LSM) coating manufactured by APS was tested at 600, 700, and 800 °C and compared with the Pyromark 2500. LSM coating, treated with laser after the deposition and before the heating tests, showed good optical properties at each temperature. LSM showed an efficiency of 0.89–0.9, equal to that of the Pyromark with α/ε values of 0.96/0.82. In this case, the selective absorber efficiency was indicated as the ratio of the net radiative energy absorbed and retained by a surface to the net radiative energy absorbed and retained by an ideal selective absorber with an absorptance of one and an emittance of zero [34]. In contrast to Pyromark paint, which showed a pronounced degradation at 800 °C and formation of secondary phase depending on the substrate, LSM experienced a drop in the absorptance up to 0.94, less than the Pyromark with 0.95, but with a lower emittance, 0.79–0.80 against 0.885 after 480 h, thus showing a better efficiency in the long term. In addition, no substrate element or secondary phases were detected after thermal treatment, pointing out the absence of reaction of coating with the substrates. Therefore, LSM is potentially more chemically stable than Pyromark over a long operating time. Despite Sandia researchers claiming the competitiveness of the plasma sprayed coatings, no further progress has been made following the reports. In addition, information is lacking on their mechanical integrity in actual use conditions, chemical and morphological features, and optimization of manufacturing processes.

As mentioned above, in contrast to coating produced by vacuum-based techniques, thermal sprayed coatings showed a heterogenous composition made by secondary phases, melted, and partially melted particles, cracks, and multiscale porosities. The synergy of these features influences the interaction of absorber material with the sun's rays. Studies have been devoted to the characterization of the optical behavior in relation to the microstructure of the coating and the manufacturing process. Brousse-Pereira and Toru [27,36] analyzed aluminum/Al₂O₃ cermet coatings manufactured by the APS process, highlighting the effect of alumina particles dispersed in the Al matrix on the optical behavior. The multiscale microstructure and multiphase nature (that can be seen as made by homogenous macro areas of single aluminum and alumina, mixed with cermet areas and porosities) lead to a complex response of the coating to the incident light, which differs from that of the homogenous material (see Figure 3).

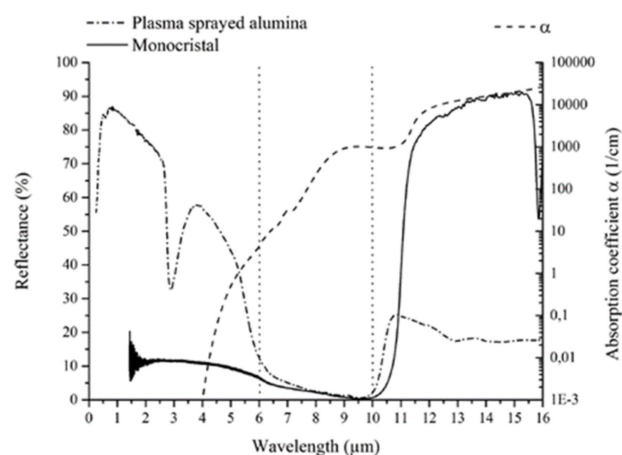


Figure 3. The reflectance of plasma sprayed alumina coating and reflectance of a single crystal of α -alumina (left axis). The absorption coefficient of α -alumina is computed from extinction index, reproduced from [27], with permission of ACS 2015.

Toru et al. [27] argued that volume scattering phenomena occurs during light/coating interaction (see Figure 4). They identified three types of phenomena: (a) diffraction, which results in a modified direction of light propagation around heterogeneity; (b) refraction that involves penetration of light in heterogeneity, along with modification of the emerging direction; and (c) multiple reflections at the interface between heterogeneity and the matrix medium. They estimated that almost 20% of solar radiation is absorbed by impurities and structural defects.

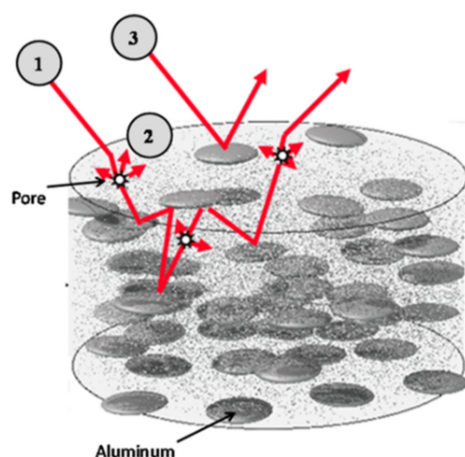


Figure 4. Illustration of scattering mechanisms that occur in cermet in the transparent region. (1) Refraction between air and alumina and multiple reflections on aluminum splats; (2) pore scattering; (3) surface reflections on aluminum splats, reproduced from [27], with permission of ACS 2015.

Brousse et al. [36] claimed that by optimizing the operating parameters and conditions (i.e., plasma power and the resultant particle in-flight speed and temperature) it is possible to obtain different microstructures and, hence, tuning the optical properties. Higher plasma power, which leads to higher processing temperature, resulted in reduced porosities (from 33% to 14%) due to the complete melting and resolidification of the particles and in a smoother surface for the material system analyzed. These features caused an increase in the reflectance of the surface from 72% to 87% in the IR range, acting more as a mirror and lowering the absorption. Low plasma power, conversely, seemed to favor the formation of a more heterogeneous structure (pores, particles with different shapes and sizes) and a rougher surface. These aspects promote the absorber efficiency: smoother surfaces are more reflective, while surface irregularities cause multiple reflections on the incident ray,

increasing the absorbed part of the radiation and decreasing the reflectance. In addition, reflectance has been found to increase with the flattening degree of the sprayed particle: a mix of globular unmelted particles and flat lamellae promotes the entrapping of the light beam within the coating and promotes the absorption of the incident radiation. Oxygen and Al_2O_3 fractions within the aluminum matrix also play a key role in the light/coating interaction. APS of Al-boehmite (AlOOH)-produced coatings have O and Al_2O_3 content up to 13% and 27% in weight, respectively. The high amount of dielectric phase dispersed in the metal phase lowered the reflectance up to 15%. In addition to these promising results, the authors also observed the importance of further investigations to understand how each phase contributes to the interaction of complex heterogeneous coating with solar radiation. Toru et al. [27] further investigated the plasma sprayed Al/ Al_2O_3 cermet in visible, NIR, and IR spectral regions (from 0.4 to 16 μm wavelengths). As also observed by Brousse et al. [36], the amount of alumina and aluminum metallic phase inside the coating has a key role in the optical behavior. In the visible–NIR spectral range (0.4–6 μm), which is of interest for solar applications, increasing the %Al in Al_2O_3 matrix increases the absorption and reduces the reflectance, but it happened in the range 0–15 wt% of Al. However, if the Al% further augments, tending toward 100%, the effect is reversed: a high fraction of easily melted metal leads to the reduction in porosities that limits the internal scattering. Therefore, increasing the aluminum fraction until a coating made by 100% of Al is obtained, the specular reflectance is promoted and the coating acts as a mirror-like surface. Conversely, low aluminum and, hence, high alumina concentrations favor a scattered reflectance, promoting the absorption of the radiation. The authors concluded that, concerning Al/ Al_2O_3 cermet, plasma spray is capable to adjust the optical properties according to the final applications.

Thermal spray processes have been adopted to deposit other material systems, e.g., perovskite oxide ($\text{La}_{1-x}\text{Sr}_x\text{TiO}_{3+\delta}$) [37], spinel structures [38], and Ni–Al alloys [39]. Zhu et al. [37] observed that, concerning perovskite, the rate of oxidation occurred during the deposition and the oxygen content in the coating, which in turn depends on the plasma power, thus influencing the reflectivity of material in the UV–visible–IR spectral range. Reflectivity is higher in coatings deposited with low plasma power (intensity current of 600–650 A) (see Figure 5). Low power led to coatings having a high fraction of unmelted particles, lower density, and high porosities (14%), and cracks. The particles, indeed, retained their initial morphology with a reduced flattening (the thickness of the lamellae was 4–5 μm) and the thicker splats favor multilayer reflection at the splat interfaces; porosities, in turn, result in a larger scattering coefficient and crystallinity degree. Conversely, in high-power plasma, particles are fully melted and the microstructure is composed of highly flattened splats (1–2 μm thick), low porosity (around 9%), and a reduced crystallinity degree, due to the higher cooling rate of the melted particles than those in low-power deposition. The authors suggested the influence of the crystallinity/amorphous state of the particle on the optical behavior, but it was not fully clarified and quantified. Oxidation also promotes reflectivity: oxygen vacancies are reduced by post-deposition heat treatment and filled by oxide scale, which acts as doping and improves the absorption [29]. The authors claimed that by optimizing temperature and the time of treatment, together with the spray process parameters, it is possible to adjust the reflectivity of the coating.

Bunmephiphit et al. [39] explored the deposition of Ni-5Al with flame spray process. The authors claimed that the Ni–Al solar absorber is a good candidate as a solar absorber material for solar collectors operating at high operating temperatures. As sprayed coatings achieve an average absorptance of 0.77 in the UV–visible–NIR range (from 0.3 to 2.5 μm), but the value was around 0.9 in the UV–visible region, and performed better than the coatings from Sandia (see Table 1) [24,25,33]. The authors suggested that it could be due to the high fraction of NiO and Al_2O_3 oxides dispersed in the Ni and Al metallic phases (no formation of intermetallic compounds, NiAl, AlNi_3 , or Al_3Ni_5 , was observed). However, this was a preliminary analysis; further strategies need to be planned to improve the absorption, and the thermal stability needs to be investigated.

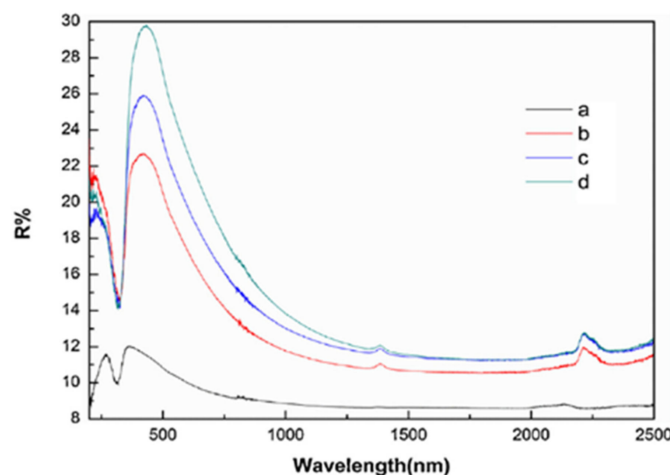


Figure 5. Reflectivity spectra of LST coatings: (a) LST-1, (b) LST-2, (c) LST-3, and (d) LST-4 (samples are listed from high to low powers), reproduced from [37], with permission of Elsevier 2015.

Most recent developments have been directed to the use of spinel structures for solar applications [40]. Indeed, they possess good intrinsic selective properties, excellent thermal stability, and oxidation resistance. Spinel coatings are usually produced by dip coating or wet coating (such as electroplating, spraying, or roll-coating [41]) that can deposit them without altering their composition or chemical structure. Deng et al. [38] investigated the production of spinel coating by means of plasma spray of vanadium tailings (VT). The high temperatures involved in the deposition process together with the oxygen-rich atmosphere promoted the reaction of feedstock particles and led to the formation of AlVO_3 and Mg_2VO_4 spinel structures and Fe_3O_4 and MnO_3 oxides. The as-sprayed coating showed remarkable optical features, with absorption in the visible range equal to 93.79%, but a higher emittance of 66.86%. In addition, the relatively high native roughness, measured at $3.8\ \mu\text{m}$, is larger than the solar radiation wavelength ($0.3\text{--}2.5\ \mu\text{m}$) and favors the multiple reflections of sunlight beams on the surface, increasing the absorption; however, it also enhances infrared emission. As observed in other coatings, reducing the roughness of spinel coatings led to a decrease in the thermal emittance but also in absorptance, with values of α/ε equal to $0.92/0.49$ and a more reflective coating. Reduction of optical properties was also observed after the thermal treatment. However, the loss in optical performance is quite low and determines an acceptable durability of the coating. Surface durability, in terms of optical properties stability, was estimated by using the PC index, defined as follows [42]:

$$\text{PC} = -\Delta\alpha + 0.25 \cdot \Delta\varepsilon$$

where $\Delta\alpha$ and $\Delta\varepsilon$ are the variation in absorptance and thermal emittance after the heat treatment, and PC must be less than 5% ($\text{PC} < 0.05$) for the absorber surface to be acceptable. Thermal spray processes have proved to be a viable solution to produce coatings that can be competitive with Pyromark paint [24,25,33,34,38]. However, many materials that are commonly used in solar applications are not suitable for deposition with thermal spray and do not represent a valid alternative; for example, pure alumina or WC-based coatings achieve low optical performance in as-sprayed conditions. For this reason, several strategies have been attempted to improve the optical properties and the selectivity of these coatings. These methods involved the production of coatings with multiscale structures, multilayered absorbers to tune the selectivity, or post-deposition treatment.

Wang et al. [26] proposed the use of blends of nano-sized and submicro-sized WC particles (0.7 and $2\ \mu\text{m}$, respectively) to create a multimodal WC-Co cermet coating utilizing HVOF process. The multimodal coating was denser and more compact: nano-sized WC particles fully melted during the process due to the high surface area with respect to the volume, and filled the pores between coarser WC particles; porosity decreased from 3%

and 2% to 1%, and a smoother surface was also obtained. The authors observed that the absorptance increased from 0.80 and 0.82 for conventional coatings (single scale WC particles) to 0.87 for multimodal. It was due to the light trapping phenomena inside the multiphase coatings, consisting of coarse and fine WC; light was reflected between the submicrometer WC particles and the uniform nanometer WC particles, resulting in more efficient light-trapping properties (Figure 6).

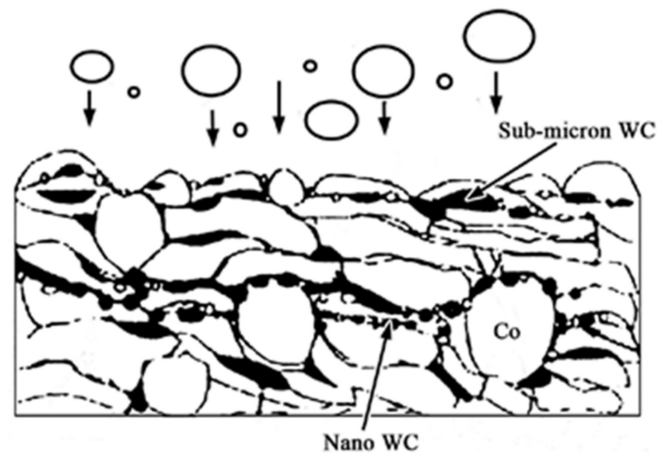


Figure 6. Sketch map of the formation of coarse and fine WC particles in the multimodal coating, adapted from [26].

Results were promising, but further optimization of the coating, including particle size range, distribution, and coating surface morphology, may be necessary to increase the absorptance, and even more, to make the thermal sprayed WC-Co competitive in solar applications. The same authors, starting from these results, explored a multilayered absorber consisting in the multimodal WC-Co absorber coating produced by HVOF, covered with CuCoMnO_x , $\text{CuCoMnO}_x + \text{SiO}_2$ spinel intermediate layer, and SiO_2 antireflective layers (ARC), deposited by dip coating to improve the absorption but also the selectivity [35].

The addition of subsequent layers on the WC-Co absorber progressively increases the absorptance. The spinel layer (composed of Cu–Mn oxides) has good intrinsic absorptance and improves the absorption of light. However, emittance also rose due to a reduction in the surface porosities; spinel particles fill the gap between unmelted round-shaped WC particles on the coating surface, making the surface smoother. The addition of the other layers, $\text{CuCoMnO}_x + \text{SiO}_2$ transition layer and SiO_2 ARC, boosted the optical performance, achieving values of α/ε of 0.915/0.290 for the final coating. The behavior is due to the beneficial effect of the SiO_2 inside the spinel structure, which acts as doping, and the gradient distribution of silicon that gradually changes the refractive index. Subsequent layers also act as protection to oxidation by providing higher thermal stability. After the annealing treatment at 500 °C, the optical properties slightly changed with α lowered to 0.901 and ε increased to 0.320. The authors argued that during the heat treatment the thermal stresses form cracks in the ARC layer and weaken the anti-reflection effect. However, the layers protect the WC/Co by diffusion of oxygen, giving the good thermal stability observed, but lower the emittance and improve the selectivity of the coating (see Figure 7).

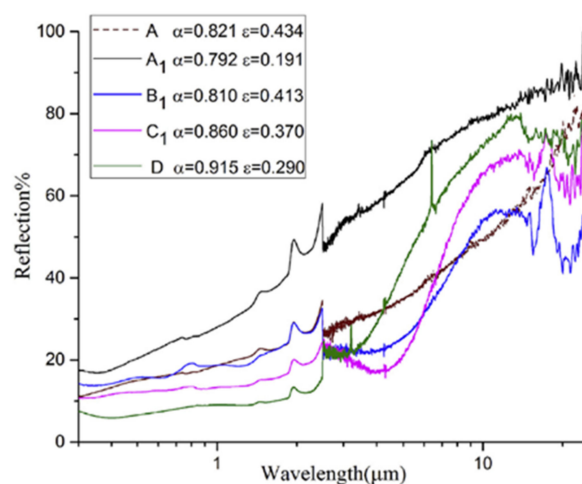


Figure 7. Reflectance curves: A—multimodal WC-Co layer; A1—polished WC-Co layer; B1—WC-Co + CuCoMnO_x layer; C1—WC-Co + CuCoMnO_x + CuCoMnO_x + SiO₂ layer; D—WC-Co + CuCoMnO_x + CuCoMnO_x + SiO₂ + SiO₂, reproduced from [35], with permission of Elsevier 2018.

A similar strategy has been proposed by Duan et al. [43] that investigated a tandem structure (see Figure 8b) made by WC/Co absorber coating manufactured by HVOF process plus an aluminum oxide (Al₂O₃) anti-reflection layer (ARC), produced by the sol-gel method. The tandem structure presents a good selectivity with α/ϵ equal to 0.908/0.145 and good stability (0.898/0.172) after annealing at 600 °C for 7 days. The observed improvements are due to the beneficial effect of Al₂O₃. Solar properties improved from 0.746/0.161 of the simple only-WC/Co to 0.827/0.145 when Al₂O₃ powders are added to the WC-Co absorber. The light-trapping effect is improved by increasing the light path inside the materials and the multiple reflections due to the heterogeneity, the multiscale inclusions effect, and alumina optimal optical properties [44,45] (see Figure 8). The ARC Al₂O₃ led to 0.852/0.153 and 0.908/0.145 for pure WC-Co and WC-Co + Al₂O₃ coatings, respectively, owing to the anti-reflection effect that the alumina coating provided for improving absorptance and reducing thermal losses.

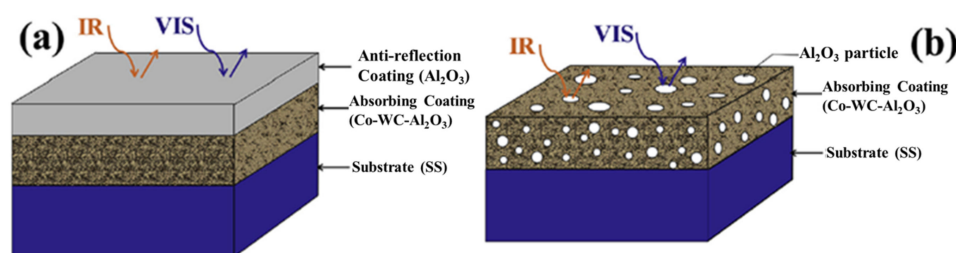


Figure 8. Schematic illustration of Co-WC-Al₂O₃ metal–dielectric composite solar selective absorbing coating: (a) double-layer composite coating; (b) single absorbing coating, reproduced from [43], with permission of Elsevier 2017.

Similar to what happened with the SiO₂ ARC in the multilayered structure developed in [35], alumina ARC prevents the diffusion of the oxygen in the underlying layer during the annealing treatment, protecting the absorber from oxidation. Cracks formed on the alumina layer lowered the anti-reflection effect, thus decreasing the optical performance, but the tandem structure showed remarkable thermal durability.

A further strategy to improve the solar absorbing properties of the thermal sprayed absorber was proposed by Gao et al. [46], which conducted post-deposition laser surface treatment on Ni–Mo and Ni–Mo–Co coatings. The purpose was to reduce the microstructure defects, correct improper surface roughness, and fix unreasonable phase contents in thermal spray coatings that cause their poor optical properties. The authors observed that

after the treatment the absorptance increased from 0.84 to 0.88 for the Ni–Mo sample and from 0.75 to 0.83 in the Ni–Mo–Co coating. It was ascribed to the complementary effect of the Ni + Mo metal volume fraction increasing from 28.6 to 47.3%, and of the reduction in the Ni-oxide content from 69.7 to 51.4%, promoted by the laser treatment. Surface roughness almost doubled after the laser process, contributing to the increase in the absorptance [47]. The work of Gao showed promise for improving the optical properties of thermal sprayed coatings by laser treatment, especially for concentrating solar power. However, despite the values reached, the proposed approach is not competitive with the usage of Pyromark, and far from the ideal threshold of 0.96.

In addition to the conventional thermal spray processes, alternative approaches have been proposed in the past that adopt cold spray [48], laser sintering [47,49], and laser cladding process [50]. Tungsten coating manufactured by laser cladding achieved an absorptance of 0.830 and a thermal emittance of 0.116 at room temperature in the as-sprayed conditions [47]. The authors argued that the significant increase in absorption of the tungsten (bulk material has α equal to 0.49) is due to the formation of tungsten oxides WO_x with various compositions having good intrinsic optical properties [51] and the multiscale surface texture, with roughness ranging from 0.5 to 1 μm . Indeed, coating absorption benefits from nano- and microroughness result from two complementary effects: (i) if the roughness is smaller than the wavelength, the surface acts as a graded-index medium exhibiting anti-reflective behavior [52,53]; (ii) when roughness is greater than radiation wavelength, multireflection occurs, favoring light entrapment. By performing a secondary laser scan on the sintered coating without adding new powders, the authors further improved the optical properties, achieving values of $\alpha/\varepsilon_{\text{room}}/\varepsilon_{80^\circ\text{C}}$ of 0.903/0.161/0.245 [49]. The coatings also showed excellent thermal stability after thermal treatment at 650 $^\circ\text{C}$ for 36 h. Absorptance slightly decreased to 0.87 and the emittance increased up to 0.49. The small variations in α/ε were ascribed to the increasing oxidation rate inside the coating with the formation of other phases (mainly iron oxides due to the steel substrate) and slight changes in the roughness; however, the protective surface oxide forming during the sintering avoids an excessive diffusion of the oxygen, retains the optical performance, and provides the high thermal stability. The FOM was estimated equal to 50, close to the performance of Pyromark 2500 paint. Pang et al. [50] manufactured TiC–Ni–Mo cermet coatings using nano-sized and micro-sized particles. The multiscale cermets proved to be valid candidates as spectrally selective coatings for high-temperature applications owing to their excellent selectivity. Cladded coatings indeed reached values of α/ε of 0.8/0.055 and 0.86/0.04 for single (only micro-sized powders of metals and ceramic were used) and multiscale coatings (using a blend of micro- and nanoparticles), respectively. Multiscale cermet benefitted from high light entrapping due to the surface morphology and the multiple interactions between nano- and microphases, as observed for the multimodal WC–Co coating [26]. Titanium carbide, having good intrinsic optical properties, also contributes to enhancing absorption in the visible range. The coatings also showed remarkable thermal stability, barely affected by the thermal cycle (see Figure 9).

From the analyzed contributions, it emerges that laser processing is a potential alternative to vacuum techniques and conventional thermal spray processes. Optimization of processing parameters and adoption of a multilayer approach, as also seen in [35,43], including, for example, anti-reflection layers, could further improve the optical properties and the selectivity. However, some doubts about the cost-effectiveness of these solutions remain undebated. Shah et al. [47] gave a rough estimation of the manufacturing cost of a laser-sintered absorber coating, showing that the technology is competitive with the vacuum process, but it refers to small receivers used in parabolic trough collectors, but the economic validity in SPT plants needs to be estimated. In addition, the in-situ usage of the laser process is not attainable. Compact plasma and cold spray process, especially in its low-pressure configuration, in contrast, are opening new scenarios for their use in solar application [54–57]. Sevillano et al. [48] explored the deposition of Ni–alumina cermet to produce coatings for solar power generation. The authors were able to produce

cermet coatings with outstanding properties, in terms of hardness, adhesion, low porosity level, and thermal stability. In addition, optical properties can benefit from the multiscale composition of the cold sprayed coating (i.e., high deformed metal particles and ceramic particles with different dimensions) derived from the fragmentation of the brittle alumina particles under the high-speed impact [48,58]. Furthermore, similar to what was observed in plasma sprayed coatings, post-deposition treatments can be beneficial to the optical properties and mechanical characteristics (e.g., surface hardness, wear resistance), which also improve the coating durability [59–62].

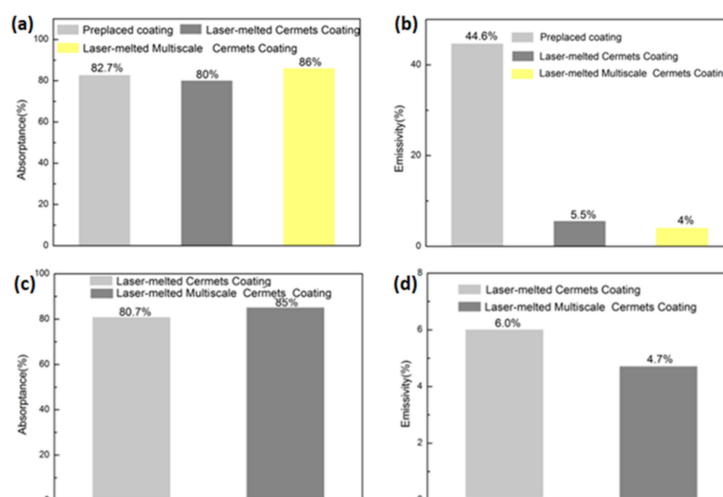


Figure 9. Absorptance and emittance of the laser-clad cermet coating: (a,b) as-produced conditions; (c,d) after heat treatment at 650 °C for 200 h (graphs are re-elaborated from [50]).

3. Thermal Spray Coatings for Molten Salt Protection

3.1. Introduction

As mentioned in the previous section, CSP technology can be efficiently integrated with thermal energy storage (TES) systems to mitigate the intermittency in solar energy and fulfill the electricity demand even during night hours. CSP technology, indeed, collects solar radiation as heat in a thermal fluid; this heat can be stored for a certain time without significant losses (the roundtrip efficiency of the TES system currently installed reaches 96% [12]) to generate electricity when required. The main benefits deriving from the integration of the TES system are related to:

- Mitigation of the intermittency of the solar energy and better matching the electricity demand; in addition, the availability of storage allows the power cycle system to operate at a constant rate achieving the highest efficiency, increasing the overall efficiency of the CSP plant;
- Transform the solar source into a dispatchable generation source of electricity—the storage allows to generate and put electricity into the grid in the period of peaks in the demand and highest prices (usually the night hours);
- Increases the annual capacity factor of the CSP plant.

On the other hand, the addition of the TES system increases the investment and the operational costs required to install and manage a fully operative CSP plant. The integration of TES systems is recommended in the case of large-scale plants operating at high temperatures: central tower plants attain more benefits from the energy storage system than the parabolic trough collector design. TES systems consist of three main parts: (i) the storage material (usually steam or molten salts), (ii) the heat transfer equipment, and (iii) the storage tanks [63,64] (see Figure 10).

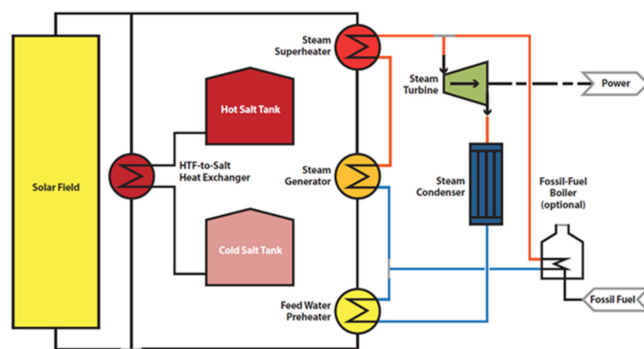


Figure 10. Scheme of a CSP system with a two-tank indirect energy storage system, hybridized with a fossil-fuel backup boiler (optional), adapted from [12].

In a TES system, the heat transfer fluid (HTF) coming from the central receiver or the parabolic trough collectors can be directly used to heat the water and generate the steam, or sent to the HTF-to-salt heat exchanger and transfer the accumulated heat to the TES fluid (usually molten salts). The TES fluid stored at low temperature in the cold tank (usually between 280 and 290 °C) is heated to the working temperature (from 380 to 550 °C, depending on the fluid used) and collected in the hot tanks. The fluid stored in the hot tank is used to heat the fluid operating in the power cycle when the solar energy coming from the solar field is insufficient to satisfy the electricity demand [64,65].

TES fluids can include water, molten salts, organic solvents, and synthetic oils. However, in practice, the choice is limited to a few suitable materials able to combine several properties, such as high heat capacity, low melting point, high boiling point, low reactivity, and thermal stability [66,67]. In the last few years, molten salts are used increasingly as heat transfer fluid for the power cycle and as heat storage media for the TES systems, being able to provide considerable advantages in terms of energy generation efficiency and allowing for higher operating temperatures, in the range of 300–500 °C up to 800 °C, depending on the salt mixture adopted [65,66,68–70]. The molten salts that are commercially available and currently implemented in CSP plants can be mixtures of nitrates and nitrites, chlorides, fluorides, or carbonates [71]. Figure 11 summarizes the salt mixture used in a CSP system and the operative range of temperature.

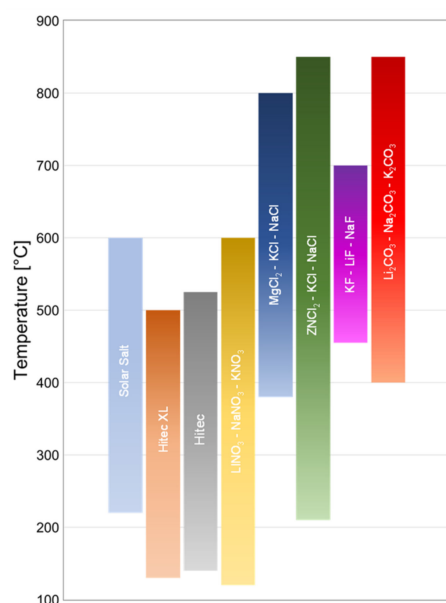


Figure 11. Melting point and maximum operative temperature of commercial molten salts (data reported from [72]).

The utilization of molten salts at higher temperatures, however, brings out challenging issues related to the compatibility with the construction materials, especially in the case of chloride salts [73–76]. CSP components, indeed, are made of metallic alloys, mainly carbon steels, stainless steels or, when required, Ni-based superalloys, which are vulnerable to corrosion attacks from HTF and TES media [14,71]. Corrosion mechanisms commonly observed in TES components are “high-temperature corrosion”, “localized corrosion” (such as pitting or cracking), and “mechanically assisted corrosion”. They are usually distinguished in “uniform” or “localized” corrosion; the first phenomenon is preferred because the rate of corrosion is usually slower and is more easily controllable, meanwhile localized corrosion phenomena are faster and could lead to an unexpected catastrophic failure of the structure [66]. Molten salt corrosion in TES involves, first, the oxidation of the metallic alloy generating protective oxide layers, and subsequently, their dissolution due to the fluxing action of the molten salts. Cyclic formation, growth, and dissolution of the oxide layer cause the continuous degradation of the metallic structure.

The occurrence of a specific corrosion mechanism strongly depends on many factors, e.g., type and composition of the alloy, corrosive medium, working conditions (i.e., temperature, atmosphere, loads, etc.), to cite a few. All influence the kinetics of the reactions and the corrosion rate. The description of the corrosion mechanisms that occur in TES system parts and the performance of the materials exposed to the different salt mixtures is too wide and beyond the main scope of the present manuscript. Readers are referred to reviews by Ibrahim et al. [72] and Walczak et al. [66]. These works provide detailed insight into the salt systems used in CSP plants and the corrosion behavior of the structural materials when exposed to molten salts.

3.2. Corrosion Resistant Coatings in TES System

Considering the susceptibility of metallic parts to corrosion when in contact with molten salts, the potential failure of TES system components represents a crucial risk for the CSP plant and a non-negligible part of the overall cost of the plant. It has been estimated that the overall impact of the TES system may reach the 25% of the initial cost of a CSP plant, where the molten salts contribute almost 50% and the components (tanks, piping, foundations, etc.) for the remaining half [77]. Preventing the failure or mitigating the damages of the TES components, therefore, can contribute to keeping the cost of reparation or of shutdown time. Several strategies to prevent or mitigate the corrosion of storage tanks have been identified in recent years; they may involve the use of a corrosion inhibitor added in the electrolyte, cathodic protection, or deposition of a protective coating having better corrosion resistance than the structural material, to cite some [78,79]. The addition of a certain amount of graphite, for example, in the nitrate salt mixture reduced the corrosion rate of carbon steel up to six times if coupled with a graphitization of the part surface [80]. The application of corrosion inhibitors was also tested to mitigate the aggressiveness of chloride salts. Mg inhibitor in MgCl_2 –KCl salt reduced the corrosion rate by 35% in Fe–Cr–Ni alloys even at the highest temperatures [81,82]. Reduction of impurities and in-service monitoring of salt purity also allow designers and engineers to control the corrosivity of molten salts [83,84]. However, these strategies are not always economically viable and, to some extent, can be detrimental to the thermal efficiency of the HTF/TES medium, compromising the overall economic effectiveness of solar energy. Coating of low-alloy structural steel, on the other hand, represents a suitable and cost-effective alternative in the design of CSP plants. Indeed, the coatings act as protective layers, avoiding the oxidation of substrate elements (especially those more prone to oxidation, such as Cr, Ni, and Al) and the depletion of the matrix of its constituents; in that way, they can enhance the lifetime of these materials by sacrificing their element during usage [85]. Usage of protective coatings has been suggested not only for low-alloyed steels but also when metals having high corrosion or oxidation resistance are used, such as stainless steel or Ni-based alloys. To serve as protection for the base alloys, compositions of the coatings have to promote oxidation of their constituents depending on the environment. The coatings should be

sufficiently dense and thick to limit the diffusion of the corrosive species through the coating before the protective oxides form [86].

First attempts to produce protective coatings concerned surface modification strategies by promoting the passivation of surface and formation of the autogenic covering layer. Gomez-Vidal et al. proposed surface passivation by means of pre-oxidation treatment of alumina-forming alloys (Al-FAs), such as Ni-based Inconel 702, Haynes 22, and Kanthal APMT [87,88]. These alloys, indeed, are prone to form on the surface a dense and protective Al_2O_3 layer having outstanding chemical and thermal stability. Alumina scales prevent the penetration of aggressive elements from the molten salt bath inside the underneath metal. The protective nature of the passivated surface derives from the formation of α - Al_2O_3 phase, but other metastable and less protective phases (γ and θ) could form in the oxidizing environment; therefore specific treatment temperatures also need to be adopted according to the specific Al-FA employed as base material. The authors tested the oxidized alumina-forming alloys with molten chlorides (MgCl_2 –KCl mixture) in both static and cycling conditions. Each alloy showed the formation of dense and uniform alumina scales (from 5 to 50 μm in thickness) during the oxidation treatment, which were able to protect the alloys from the molten chlorides under 700 °C isothermal conditions. The composition of the base material was found to influence the corrosion resistance; the large amount of Ni in the Inconel 702 seemed to decrease the corrosion, while other elements, such as Fe, Al, Cr, Ti, and Mo were more prone to dissolve in molten salts. In thermal cycling conditions from 550 to 700 °C, the alumina layers behaved similarly for short time exposure; in the case of long-term exposure, they became unstable, especially in the inert atmosphere—Al depleted from the alloys and the scales spalled, enabling the alumina to reform due to the reduced amount of oxygen, and exposing the metallic surface to the corrosive molten chlorides. The results proposed by the authors seem promising and suggest that the approach is a viable strategy for corrosion mitigation in CSP. In addition, the possibility of using an oxygen-rich atmosphere instead of an inert one makes it more commercially feasible. However, the methodology does not seem sufficiently developed to be implemented in actual plants, and some concerns need to be addressed. In short-term tests, the alumina layer remains stable and the corrosion is uniform and, thus, controllable; however, in long exposure, the alumina layers and the underneath metals could experience localized corrosion and intergranular attack due to the depletion of constituent elements, especially the Cr-rich alloys, which can lead to a catastrophic failure of the coating. The formation of a metastable phase of alumina during the oxidation can also cause the formation of internal cracks, promoting a stress-cracking-corrosion (SCC) mechanism. Therefore, particular care needs to be taken during the oxidation treatment to establish proper conditions, which is not always achievable. This, together with the adoption of costly alloys, could impact the overall cost of the TES system. Finally, despite the use of an oxygen-rich environment that can favor the performance of the Al-FA, chloride gases (usually form over the liquid bath) can combine with oxygen and produce a harsh and highly aggressive atmosphere; therefore, the mitigation strategy needs to take into account the protection of the surface exposed to the liquid salt and the surface exposed to the chloride vapors.

The early published literature focused on the corrosion-resistant thermal sprayed coatings for conventional energy generation plants or engine components, such as turbine blades or heat exchangers, while the protection against nitrate, chloride, or carbonate salts in solar energy plants has not been explicitly considered at the beginning. However, these studies shed light on the behavior of the materials (not only as bulk but also as strongly heterogeneous systems) under those aggressive conditions, and their outcomes can be transferred to design production methodology to be adopted in solar energy applications.

First experimentations on the use of thermal spray coatings as a protective layer were directed toward the development of thermal barrier coating (TBC) in power generation components, namely cell fuels, incinerators, fossil boilers [85,89,90], or high-temperature steam tanks [91,92]. Other applications of these coatings may be anti-corrosion barriers for aeronautical gas turbines [93–95] and high-power diesel engines [96]. In those systems,

the combustion of fuels leads to the formation of ashes (which are mainly compounds of sulfur-, vanadium-, sodium-, or potassium-forming chlorides, sulfides, etc., depending on the fuel used) on the surface of the metallic parts. These salts are deposited on the surfaces in a molten state due to the high operating temperatures (above the melting point of the salts); in an oxidation environment, they react with the metals and trigger the corrosive attack, leading to the dissolution of the native protective oxide and then promoting the transport of the oxidizing species inside the metallic part. Aguero et al. [89] tested the corrosion resistance of Al–Co–Fe–Cr (57–18–13–11 wt%), Ni–Al (80–20 wt%), and Fe–Cr–Al (60–30–5) deposited by atmospheric plasma spray and HVOF, in molten carbonate ($\text{Li}_2\text{CO}_3 + \text{K}_2\text{CO}_3$) at 700 °C. The authors observed that Cr-rich ferrous plasma spray coatings performed well as protective layers, remaining stable even after long exposure (1000 h) with no significant alteration of the starting composition and avoiding the substrate to be attacked by the corrosive agent. The improved corrosion resistance was ascribed to the iron–aluminide (FeAl) compounds and aluminum oxide scales formed in the coating during the deposition. Conversely, NiAl does not form protective nickel aluminides and shows unalloyed elements, close to the nominal composition of the powders, in the coating. It led to poor corrosion resistance of the coating and, consequently, the substrate attacked after 300 h of exposition. The study does not provide a quantitative analysis of the corrosion rate or the penetration of corrosion through the thickness of the coating; however, in the authors' opinion, thermal spraying can be a viable technology to improve the resistance of fuel cell components depositing a protective coating without requiring expensive heat treatments, and with better performance and lower costs than the conventional aluminide coatings manufactured by ion vapor deposition. Senderowsky et al. [97] also investigated the corrosion of FeAl intermetallic-based coatings against sodium-based molten salts (Na_2SO_4) at 850 °C. Iron aluminides were produced by depositing four different powder systems, namely pre-alloyed Fe40Al, Fe25Cr + FeAl–TiAl– Al_2O_3 mixture, Fe46Al–6.55Si (at%) and multiphase Fe_xAl_y , by HVOF facility. The authors observed that the different composition and morphology of the initial mixtures affected the microstructure and the resultant behavior as thermal barrier of the coatings. The first mixture led to the formation of the stoichiometric intermetallic compounds of Fe and Al and Fe- and Al-oxides (only $\alpha\text{-Al}_2\text{O}_3$) within the coating that gave higher corrosion resistance. In the other coatings, additional systems in the mixtures led to a pronounced heterogeneity in the chemical composition and the phases; the authors observed the presence of the other nonprotective alumina phases, i.e., γ -, θ - and $\delta\text{-Al}_2\text{O}_3$, and different aluminides compounds in the Fe_xAl_y coating that suffered severe damages and showed a loss in integrity and a decohesion from the substrate with a consequent acceleration in the corrosion rate. The depletion of aluminum in the FeAl matrix resulting from the formation of the aluminum oxide scales; in addition, this favored the development of FeS sulfides that infiltrated the thickness through the particle boundaries and reached the substrate. Ti-added and Si-added coatings, despite a slightly better resistance to the molten salts than the multiphase coating, experienced a severe intergranular corrosion localized at the splat boundaries due to the presence of cracks and SiO oxide at the particle boundaries.

FeAl intermetallic coatings can provide good protection in aggressive salts, but not per se; their performances are, indeed, very sensitive to the processing conditions and their morphologies, and particular attention has to be given to the choice of the starting materials and the processing method.

Aluminide-based coatings have also been investigated [98–100]. In these works, the authors deposited the aluminides by slurry spray process. Pure, iron- and nickel–aluminide coatings were tested with solar salt mixture, Na/K/Li carbonates, and Na/K chlorides. Slurry spraying, indeed, represents a low cost and practical method to apply several types of coatings on a great variety of surfaces, even the inner surface of tubes [99]. Samples were tested in both static and dynamic regimes at temperatures resembling the actual operating conditions, namely 580 °C for nitrates, 650 °C for carbonates, and 700 °C for chlorides. Regardless of the molten salts used to test the aluminide coatings, all systems

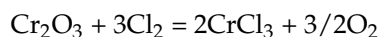
showed better performance than uncoated substrates. Concerning solar salt molten nitrates, aluminide and nickel–aluminide coatings did not show any remarkable microstructural change, even after long exposure, and no differences in their behavior were observed in static and dynamic conditions. It suggests that aluminides have excellent stability with nitrate at those working loads. Nickel–aluminide showed better corrosion resistance owing to the formation of a Ni- and Al-rich oxide layer on top of the coating. These stable oxides formed after the post-deposition heat treatment was applied to the coated system and required to dry and consolidate the slurry coating on the substrate [98]. Iron–aluminides also proved to be able to prevent the corrosion of substrate when exposed to molten carbonate salts; substrate passed from a corrosion rate of almost 2500 $\mu\text{m}/\text{y}$ in the uncoated conditions to being unaffected when coated. However, in this case, the coating suffered severe corrosion with almost 90% of the thickness oxidized after 1000 h of exposure. Furthermore, the corrosive attack appeared to be more extended over the coating under dynamic conditions, with deeper penetration of the corrosion products. The main issue observed in the system tested, however, related to the nonuniform corrosion experienced by the coatings in static and dynamic tests, which can lead to an unpredictable progression of corrosion over a longer time. The authors noted that the problem occurred due to the low and nonuniform percentage of aluminum within the slurry and suggested the necessity of further investigations considering a greater amount of Al in the aluminide, which may allow the formation and duration of the Al-oxide protective scales.

From an industrial point of view, slurry aluminide coatings could represent a viable solution for the mitigation of corrosion in CSP/TES components. The process, indeed, allows for easily coating wide and complex surfaces (e.g., inner surface of storage tank or internal surface of tubes). However, slurry spray usually requires a secondary deposition process, such as electrodeposition [98] and a post-deposition treatment, usually a diffusion heat treatment at high temperature (around 700 and 1100 $^{\circ}\text{C}$, depending on the materials) and controlled atmosphere (usually low in oxygen), necessary to consolidate the coating on the substrate and promote the formation of protective stable Fe-, Al-, and Ni-based oxide compounds [98,99]. This occurrence limits use of this method to small/medium-sized components, increases the processing time, and prevents its use for in situ maintenance and repair of worn parts. In this scenario, thermal spray processes, especially in their compact versions, can be a better alternative. In addition, several concerns arise concerning the mechanical strength of the slurry sprayed coatings when exposed to corrosive ambient and their stability, which have not yet been exhaustively investigated. Degradation in mechanical properties in harsh environments, indeed, can trigger SSC phenomena as a combination of intergranular attack mechanism and creep.

Further experimentations have been oriented toward the development of Ni-based alloy coatings, aiming to exploit their outstanding corrosion resistance with molten salts [76,101–104]. Ni_3Al aluminide coatings were produced by using atmospheric plasma spray starting from separated Ni and Al powders and exposed to a sodium–vanadium salt mixture at 900 $^{\circ}\text{C}$ [85] under cyclic conditions. Despite what has been observed by [89], Ni_3Al coating showed compact and intact oxide scales made of Al_2O_3 and NiAl_2O_4 spinel (both more protective) dispersed in a less-protective NiO main phase. The authors did not observe significant corrosion through the thickness of the Ni_3Al coating and after the corrosion cycles, it successfully remained adherent to the substrate that in turn did not show any remarkable traces of oxidation. The oxides, formed at splat boundaries, reduce the porosities and make the coating denser, slowing the diffusion of the aggressive elements from the molten salt bath. Formation of the oxide scales progressively occurs during the corrosion cycles leading to a high corrosion rate at the beginning, which decreases as these oxides stabilized. The uncoated substrate (Ni-based alloy Superni 75) experienced a continuous cycle of formation and spallation of oxide scales during the hot corrosion that causes the degradation of the materials. Tristanco-Reyes et al. [90,105] studied the behavior of NiCrFeNbMoTiAl coating deposited by plasma spray on the low-grade T22 steel with sodium–vanadium (80% V_2O_5 –20% Na_2SO_4 and 80% Na_2SO_4 –20% V_2O_5 mixtures)

and potassium–vanadium (80%K₂SO₄–20%V₂O₅) molten salts. Depending on the salts and on the temperatures, the coating showed different behaviors but performed well with values of corrosion rate far lower than the uncoated T22 steel. Corrosion rate of 0.843 and 0.150 mm/y for 80%V₂O₅–20%Na₂SO₄ and 80%V₂O₅–20%K₂SO₄, respectively, were measured. When the coating was exposed to 80%V₂O₅–20%Na₂SO₄, the corrosion rate increased from 0.494 to 0.5191 and 0.933 mm/y when salt temperature was set at 700, 800, and 900 °C, respectively. The values measured are still too high to be accepted in the TES system, but the deposition process was not optimized, and the thermal conditions were more severe than those applied in hot tanks. The results are promising and can lead the way to the use of low-alloy steel in both cold and hot tanks, replacing the more expensive stainless steels and Ni-alloys.

Ni–Cr systems have also been studied as protective coatings; nickel and chromium form highly stable oxides when exposed to an oxidizing environment, providing high resistance to aggressive media. A thorough study was conducted by Porcayo-Calderon [106,107] on the performance of Ni20Cr coating deposited by HVOF and combustion powder spray processes with chloride salts. Regarding the chloride salt, the authors observed that coating performed better than the uncoated stainless steel 304 substrate, especially at high temperature. At a temperature of 350 °C, steel and Ni20Cr behaved similarly; the exposure to the chlorides promoted initial corrosion and the formation of a stable layer of chromium oxide (Cr₂O₃) that prevented further aggressive actions. At higher temperatures (from 400 to 450 °C), however, 304SS experienced severe corrosion that led to rapid degradation of the material. The authors suggested that the “active oxidation” mechanism is established when the temperature of molten chlorides rose above a threshold. During active oxidation, the protective FeO_x and CrO_x dissolved in the salt, forming FeCl_x and CrCl_x gases according to the following reaction:



The gaseous metallic chlorides penetrate quickly in the material through the interconnected voids, and porosities formed after the depletion of Fe and Cr elements inside the material (bulk and coating), driven by physical transportation phenomena, which are faster than a solid diffusion mechanism. The metallic chlorides react with oxygen forming nonprotective Fe/CrO_x oxides and Cl₂. The high concentration of Cl₂ triggers again the degradation cycle, leading to poor adherence of the oxide scales formed on the steel, which spall and expose the surface to the aggressive medium [108,109]. Conversely, Ni20Cr in both conditions remains stable without significant degradation and only slight penetration of the salts through the surface porosity. Only at the highest temperature does the coating experience a more pronounced degradation due to the preferential attack by chlorides to chromium oxide, which causes the formation of cracks inside the coatings. NiO is more stable and less soluble in chlorides than Fe and Cr, despite CrO_x usually being more protective than Fe and Ni oxides. Additionally, NiCl_x is more thermodynamically stable and conditions to dissolve in oxide do not establish. The presence of Ni, more than Cr, in the coating contributes to the globally higher resistance of the coating compared to Fe- and Cr-rich alloys [110]. HVOF, therefore, can be addressed as a suitable technology to manufacture protective coatings in TES applications. However, corrosion protection in molten salts does not only depend on the material per se, or on the morphology of the manufactured coating, but is strongly influenced by the chemical stability of the metallic element and their compounds, such as oxides and chlorides. Contributions of [106,107] provide a beneficial understanding of the behavior of Ni-, Cr- and Fe-based alloy and open the way to further improvements related to the investigation of coating stability at higher operating temperatures (closer to the CSP regime) and the optimization of the thermal spray deposition.

Flame sprayed Ni20Cr coating provided good protection against V₂O₅–NaSO₄ molten salt mixtures up to 750 °C [111]. The corrosion velocity was found susceptible with the temperature and exposure time. The corrosion rate is highest at the beginning (namely 1–2 h)

and no remarkable differences are visible between the coated and the uncoated 312SS. After a long exposure, i.e., 22 h, NiCr coating experienced severe corrosion but was able to resist much more than the uncoated steel, retarding the corrosive attack. Corrosion rate established around 15,000 mpy at 750 °C while the steel showed almost 40,000 mpy. The coating reduces the steel corrosion rate. When uncoated, it is by more than 50%; however, the value is still high for practical applications in CSP and needs more study before protection against this corrosive phenomenon can be recommended.

In very recent works, Gomez-Vidal et al. [112,113] proposed the use of MCrAlX (where M is Ni or Co; X stands for Y, Hf, Si, or Ta) compounds deposited by HVOF or APS with carbonate and chloride salts ($\text{KCO}_3\text{--Na}_2\text{CO}_3$ (46.2/53.8 wt%) and $\text{KNa}_2\text{CO}_3\text{--Li}_2\text{CO}_3$ (33.4/34.5/32.1 wt%) mixtures. These alloys were successfully used to protect the surface of turbine blades from molten salt attacks. The protective effect derives from the formation of a compact and fully adhered alumina layer on the coating surface when exposed to an oxidizing environment, which provides high-temperature corrosion resistance [114–116]. The authors investigated different MCrAlX systems (that have already been used as a bond coat in thermal barrier coating) having distinct compositions (Figure 12 summarizes the corrosion rate of the coatings and the uncoated substrate used as a benchmark). As expected, uncoated alloys suffered severe corrosion at all temperatures, with values of corrosion rate ranging from 0.5 mm/y at 650 °C to more than 2.5 mm/y at 700 °C. Alloys with high Ni%, such as In800H and SS310, showed better resistance than other high-grade alloys, namely 321 and 347 stainless steel and In625.

All the coatings allowed for reducing the corrosion rate to a minimum of 34 $\mu\text{m}/\text{y}$. APS coating Ni–Co–Cr–Al–Hf–Si–Y showed the best corrosion resistance after a pre-oxidation treatment, passing from approximately 1 mm/y of the as-deposited coating to 34 $\mu\text{m}/\text{y}$. It was followed by HVOF coating Co–Ni–Cr–Al–5Y that achieved a corrosion rate of 46 $\mu\text{m}/\text{y}$ after oxidation. Such behavior was also observed with chloride salt mixture (44.53 wt% NaCl–55.47 wt% KCl). Uncoated alloys were severely attacked by chlorides with 2.5 and 4.5 mm/y measured corrosion rate. Thermal sprayed coatings reduced the corrosion rate by one order of magnitude, except for the NiCrAl system, which registered values at 570 $\mu\text{m}/\text{y}$ for NiCoCrAlYTa, 980 $\mu\text{m}/\text{y}$ for NiCo–CrAlYHfSi, 1230 $\mu\text{m}/\text{y}$ for NiCoCrAlY, and 1240 $\mu\text{m}/\text{y}$ for NiAl in as-deposited conditions. High percentages of Ni in the coating composition are beneficial to the corrosion resistance with chloride salts; indeed native Ni-oxide formed during the HVOF/APS deposition process is more stable than Cr and Fe oxides and slows the “active oxidation” mechanism [108,109].

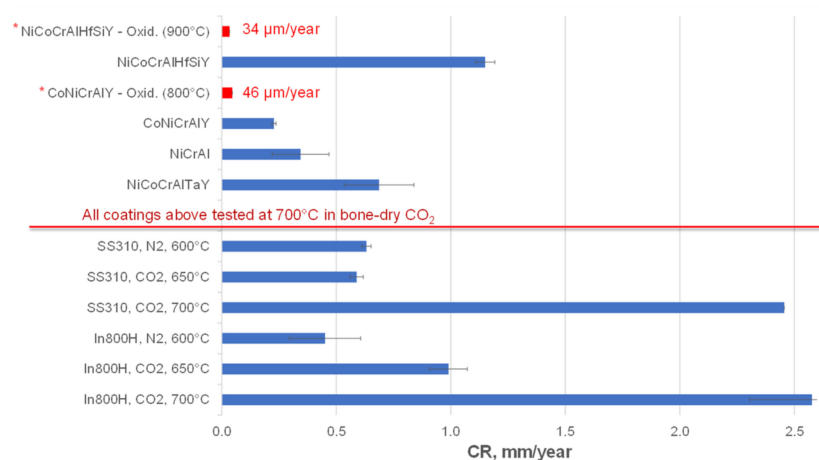


Figure 12. Corrosion rates of bare and coated alloys in $\text{Na}_2\text{CO}_3\text{--K}_2\text{CO}_3\text{--Li}_2\text{CO}_3$ in bone-dry CO_2 and N_2 atmospheres, reproduced from [113], with permission of Elsevier 2016.

Pre-oxidation treatment further decreases the corrosion for all coatings. HVOF sprayed NiCoCrAlYTa reached a corrosion rate of 190 $\mu\text{m}/\text{y}$ reducing the corrosion of SS310 substrate by 96%. Coatings form corrosion products when exposed to the salts on the

surface and through the thickness, at the interface with oxide scales formed after pre-oxidation treatment, and near residual pores generated during the thermal spraying (see Figure 13 and Table 2). These products, rich in Al and Cr-oxides, did not propagate deep within the coating and remain confined near the surface; the pores are not interconnected and prevent the permeation of the molten salts through the coating to the substrate, which did not show evidence of corrosion attacks.

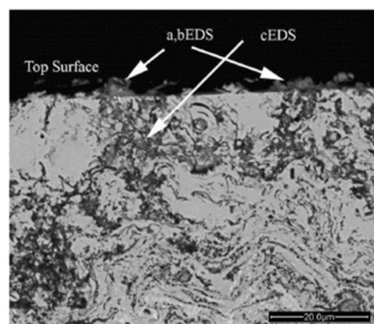


Figure 13. BSE-SEM image of pre-oxidized HVOF-NiCoCrAlYTa (air, 900 °C, 24 h, 0.5 °C/min) and exposed to NaCl-KCl at 700 °C, showing penetration at the outer surface of the top coating, adapted from [112].

Table 2. Element percentage from EDS analysis of HVOF-NiCoCrAlYTa pre-oxidized surface after exposure to NaCl-KCl salt (see Figure 13), data from [112].

EDS wt%	Phase		
	a	b	c
O	22.76	31.24	20.12
Al	0.33	2.19	26.08
Si	0.79	1.00	1.15
Cr	48.21	50.09	16.82
Fe	1.10	1.18	0.58
Co	5.48	2.28	12.54
Ni	10.81	2.70	20.58
Y	8.56	7.09	0.51

Corrosion performance depends on the composition of the coatings but also on the manufacturing processes. The pre-oxidation favored the formation of a protective alumina layer (almost 3 μm thick) on the surface of the coating, which separates the metals from the carbonates reducing the corrosion. It can result in a reduction of 50% w.r.t. the as-sprayed coatings. However, heating conditions that are too extreme could be detrimental to corrosion resistance. HVOF sprayed NiCoCrAlYTa, pre-oxidized at 1000 °C, indeed, showed a higher corrosion rate than as-deposited coating; the authors argued that treatment was too close to the maximum operating temperature of the materials (around 1050 °C), leading to a loss of cohesion of particles inside the coating, which accelerated the corrosion. Additionally, both thermal spray process and pre-oxidation altered the substrate; refinement of grains at the coating/substrate interface, precipitates (AlN), depletion of Cr (for the SS), boundary ditching, and sensitization due to Cr-carbide precipitation have been observed. These can promote intergranular attack and the occurrence of localized corrosion (pitting) in the substrate if the coating fails in protecting it.

A novel approach proposed by [117] employed amorphous Fe-Cr (60Fe-40Cr) and Ni-Cr (60Ni30Cr5Mo and 60Ni40Cr) coatings, deposited by diamond jet spray as protection against molten chlorides. The absence of grain boundaries and the lack of crystal defects in the amorphous microstructure, indeed, should prevent the intergranular attack, occurring due to the dissolution of chromium in chloride solution in Cr-rich alloys, and increase the corrosion resistance [118]. Manufactured coatings performed well, not show-

ing remarkable corrosion and protecting the substrate from chloride attacks. Coatings experienced neither a significant degradation nor Cr depletion, despite the amount of chromium present in their composition. The authors ascribed the observed behavior to microstructure recrystallization of the coating after exposure to molten salt at 750 °C; they suggested that crystallization could inhibit the interaction between Cr and chlorides, thus enhancing the corrosion resistance, but the mechanisms behind the low degree of corrosive attack were not fully clarified.

Outcomes of the work by Gomez-Vidal and Raiman indicate that protection by the thermal spray deposition of high-resistant coatings is a viable approach to extend the use of carbonates and chlorides for a TES system, allowing an increase of the operating temperature from 550 °C (the actual operative limit to employ the nitrates mixtures) to 700/750 °C. Increasing the operating temperature regime, use of low-cost HTF/TES fluid (at least in case of chlorides), and reduction in the plant maintenance and shutdown costs, derived from a longer lifetime of the components, make more achievable the goal of the Strategic Energy Technology (SET) plan and the DOE SunShot program, which aim to reduce the levelized cost of energy (LCOE) of a solar source and to increase penetration of solar energy into the energy system [119,120]. However, to date, more studies are required; deposition processes are not fully optimized, and the solutions proposed were mostly tested in very controlled, laboratory-scale conditions (inert atmosphere static exposure, and high purity). Information on the behavior of these protective coatings for in-service conditions lacks the following: testing in flowing salts to exclude saturation of salt with a thermal gradient, investigating salts with a range of chemistries (including salts with impurities and redox additive), and analyzing reactive atmospheres. All are necessary, however, to fully determine the performance of the protective coatings and predict their duration.

4. Conclusions and Future Perspectives

The next generation of concentrating solar power plants is expected to work at higher temperatures, from 600 °C for actual generation up to 850 °C or more, in order to achieve higher efficiency. In this regard, one of the main goals for engineers and designers is to increase the amount of energy collected from solar radiation, maximizing the heat delivered to the transfer fluid and, at simultaneously, reducing the heat loss at the receiver. Currently, the use of absorbing coatings manufactured by thermal spray techniques has been shown as a viable alternative, a compromise between vacuum processes (e.g., PVD, CVD, etc.) and wet chemistry technologies (such as sol-gel dip coating or painting). Thermal spray processes, indeed, provide intriguing advantages, such as high stability of the coating, very good mechanical performance, high production efficiency with relatively low capital cost, and ease of scaling from small to large production volumes. In the last decade, several attempts have been made to extend the use of thermal spraying from conventional surface modification applications to the manufacturing of selective absorbers. The thermal sprayed cermet coating showed values of optical properties below those achievable with vacuum processes and far from the Pyromark 2500 paint target, with absorptance not above 0.85 and thermal emittance at approximately 0.4 or higher. The main reason behind the observed results is related to the strong heterogeneity of the coatings deposited by thermal spraying; thermal sprayed coatings, indeed, are characterized by a complex microstructure made by flat lamellae and partially melted particles, and by open and closed porosities. Porosities, grain boundaries, internal phases, and surface roughness influence the interaction between the incident light and the material conditioning the final optical properties. In addition, the contributions reviewed show that slight variations in process parameters may have a significant effect on optical performances, more than those observed on other properties, e.g., mechanical, geometrical, or morphological. The strategies explored to make thermal sprayed absorbers more competitive involve post-deposition processing, mainly heat treatment, to promote the formation of specific oxide phases on the coating surface, or multimodal structures obtained by adding in the metal matrix reinforcement, having distinct sizes from nano- to microscale, or the use of multilayered coatings. These solutions

successfully improve the optical properties of sprayed coatings, raising the absorptance to 0.9 or more, and with reduced values of emittance. Conversely, they add complexities to the manufacturing of the coating, and further operative costs. The efforts of the research reviewed here lead the way to the diffusion of thermal spray in the CSP technologies, especially for the solar tower systems, where the large scale of the plants and challenging operating conditions make these processes very intriguing. However, more work is still needed. First, thermal spray processes have been widely optimized for a great variety of materials and several applications, such as thermal and electromagnetic barriers and wear and corrosion resistance, but the interaction between process and optical performance has only been marginally investigated; more research is necessary for the solar-absorbing materials. Furthermore, the data collected from these experimentations are related to laboratory measurements in very controlled conditions; analyses of coating performance and durability in actual operative conditions (thermal and mechanical cycling stresses, variable night-and-day solar exposure, harsh environments, etc.) are lacking in the current literature and need to be implemented in order to assess the feasibility of thermal spraying.

Significant improvements in the diffusion of concentrating solar power plants can also derive from the development of thermal energy storage technologies. In this field, research is oriented to new materials for both thermal-energy-storage fluids and storage tanks, able to withstand increasingly higher operating temperatures. In this scenario, the use of molten salts as a heat transfer fluid or as an energy storage medium has been proposed in order to reach working temperatures between 600 and 800 °C. However, the use of such aggressive media at those temperatures leads to severe issues related to the integrity of the structural components (namely, piping, heat exchangers, and storage tanks) of concentrating solar power and thermal energy storage systems, due to the vulnerability of the construction materials against the corrosive attacks from the molten salts. The way proposed recently by designers and producers to prevent the critical failures or mitigate damages in thermal energy storage and concentrating solar power components involves the use of low-alloyed structural steels coated with high resistant materials. Coatings, indeed, act as a protective barrier limiting or slowing the oxidation reactions of the constitutive elements of the substrate, and self-sacrificing to prevent damage to the components. Thermal spray processes have been employed since the 1980s to manufacture corrosion protective coatings in energy generation plants and engine components, and a wide and exhaustive literature can be found. However, protection against nitrate, chloride, or carbonate salts in solar energy plants by using thermally sprayed coatings has been marginally debated, and only in the last decade devoted investigations have been conducted. To date, it is not possible to derive a direct comparison between the coatings because the measured performances are susceptible to the test conditions (time and temperatures, mainly), the type of test, and the analysis methodology. However, the published contributions indicate that thermal sprayed coatings successfully protect the substrate from corrosion, even if they suffered severe degradation. In some circumstances, the coatings showed a corrosion rate of around 30 to 40 $\mu\text{m}/\text{y}$ in very severe conditions, almost matching the value of 10 $\mu\text{m}/\text{y}$, suggesting this as the threshold to guarantee an uninterrupted 30-year working life of the plant. In other examples, coatings registered a very high corrosion rate (even exceeding 1 mm/y), but they always performed better than the uncoated substrate in the same conditions, and in all cases, no traces of degradation were detected in the substrate. The results depicted by the revised contributions are promising and suggest that thermal spray deposition of highly resistant coatings is a suitable approach for corrosion protection of thermal energy storage components, not only with nitrates but also with carbonates and chlorides, allowing an increase in operating temperature from 550 °C (the actual operative limit to employ the nitrates mixtures) to 700/750 °C. However, more studies are needed. Indeed, the solutions proposed were mostly tested in very controlled, laboratory-scale conditions (inert atmosphere, isothermal and static exposure, and high purity of salts). The behaviors observed are valid for the specific coating/corrosive medium pair and are related to the particular conditions; therefore, predictions concerning the performance of coatings

and their duration are not fully reliable. In addition, estimates of corrosion behavior of the coatings have been made, hypothesizing the occurrence of uniform corrosion of the coating that is a safe condition, while localized corrosion phenomena (pitting or crevice formation), which can lead to a catastrophic and premature failure, have been neglected in a first approximation. Furthermore, information about the behavior of these protective coatings for in-service conditions needs to be collected. Tests involving flowing salts, which more closely resembles what actually occurs in thermal energy storage facilities and concentrating solar power plants, and including salt saturation and salts with a range of chemistries (i.e., impurities or redox additives) together with variable thermal gradients and a reactive atmosphere, need to be carried out.

Author Contributions: Conceptualization, P.P. and G.P.; methodology, F.R. and P.P.; formal analysis, F.R.; investigation, F.R. and G.P.; resources, P.P.; data curation, G.P.; writing—original draft preparation, F.R.; writing—review and editing, F.R., G.P., P.P., and P.C.; supervision, P.P.; funding acquisition, F.R. All authors have read and agreed to the published version of the manuscript.

Funding: The authors wish to thank “Comunidad de Madrid” and European Structural Funds for their financial support to the ACES2030-CM project (S2018/EMT-4319).

Institutional Review Board Statement: Not applicable.

Informed Consent Statement: Not applicable.

Data Availability Statement: Not applicable.

Acknowledgments: This project received funding from the European Union’s Horizon 2020 research and innovation programme under the Marie Skłodowska-Curie grant agreement No. 754382.



Conflicts of Interest: The authors declare no conflict of interest.

Disclaimer: The content of this article does not reflect the official opinion of the European Union. Responsibility for the information and views expressed herein lies entirely with the authors.

References

1. Ho, C.K.; Iverson, B.D. Review of High-Temperature Central Receiver Designs for Concentrating Solar Power. *Renew. Sustain. Energy Rev.* **2014**, *29*, 835–846. [\[CrossRef\]](#)
2. Epstein, M.; Liebermann, D.; Rosh, M.; Shor, A.J. Solar Testing of 2 MWth Water/Steam Receiver at the Weizmann Institute Solar Tower. *Sol. Energy Mater.* **1991**, *24*, 265–278. [\[CrossRef\]](#)
3. Pacheco, J.E.; Bradshaw, R.W.; Dawson, D.B.; De la Rosa, W.; Gilbert, R.; Goods, S.H. *Final Test and Evaluation Results from the Solar Two Project*; SAND2002-0120; Sandia National Laboratories: Albuquerque, NM, USA, 2002; pp. 1–294.
4. Forsberg, C.W.; Peterson, P.F.; Zhao, H. High-Temperature Liquid-Fluoride-Salt Closed-Brayton-Cycle Solar Power Towers. *J. Sol. Energy Eng.* **2007**, *129*, 141–146. [\[CrossRef\]](#)
5. Schiel, W.J.C.; Geyer, M.A. Testing an External Sodium Receiver up to Heat Fluxes of 2.5 MW/M²: Results and Conclusions from the IEA-SSPS High Flux Experiment Conducted at the Central Receiver System of the Plataforma Solar de Almeria (Spain). *Sol. Energy* **1988**, *41*, 255–265. [\[CrossRef\]](#)
6. Rovense, F.; Reyes-Belmonte, M.Á.; Romero, M.; González-Aguilar, J. Combined Heat/Cooling and Power Generation Using Hybrid Micro Gas Turbine in a CST Plant for a Residential off-Grid Application. *AIP Conf. Proc.* **2020**, *2303*, 080006. [\[CrossRef\]](#)
7. Chen, R.; Romero, M.; González-Aguilar, J.; Rovense, F.; Rao, Z.; Liao, S. Design and Off-Design Performance Comparison of Supercritical Carbon Dioxide Brayton Cycles for Particle-Based High Temperature Concentrating Solar Power Plants. *Energy Convers. Manag.* **2021**, *232*, 113870. [\[CrossRef\]](#)
8. Poullikkas, A.; Rouvas, C.; Hadjipaschalis, I.; Kourtis, G. Optimum Sizing of Steam Turbines for Concentrated Solar Power Plants. *Int. J. Energy Environ.* **2012**, *3*, 9–18.
9. Rovense, F.; Reyes-Belmonte, M.A.; González-Aguilar, J.; Amelio, M.; Bova, S.; Romero, M. Application of Un-Fired Closed Brayton Cycle with Mass Flow Regulation and Particles-Based Thermal Energy Storage Systems for CSP. *AIP Conf. Proc.* **2019**, *2126*, 030047. [\[CrossRef\]](#)

10. Rovense, F.; Reyes-Belmonte, M.A.; González-Aguilar, J.; Amelio, M.; Bova, S.; Romero, M. Flexible Electricity Dispatch for CSP Plant Using Un-Fired Closed Air Brayton Cycle with Particles Based Thermal Energy Storage System. *Energy* **2019**, *173*, 971–984. [CrossRef]
11. Quaschnig, V.; Geuder, N.; Richter, C.; Trieb, F. Contribution of Concentrated Solar Thermal Power For A Competitive Sustainable Energy Supply. Clean Air 2003, Lisbon. Available online: <https://www.volker-quaschnig.de/downloads/CleanAir2003.pdf> (accessed on 11 June 2021).
12. MIT Energy Initiative. *The Future of Solar Energy*; MIT Energy Initiative: Cambridge, MA, USA, 2015.
13. Rovense, F.; Amelio, M.; Scornaienchi, N.M.; Ferraro, V. Performance Analysis of a Solar-Only Gas Micro Turbine, with Mass Flow Control. *Energy Procedia* **2017**, *126*, 675–682. [CrossRef]
14. Islam, M.T.; Huda, N.; Abdullah, A.B.; Saidur, R. A Comprehensive Review of State-of-the-Art Concentrating Solar Power (CSP) Technologies: Current Status and Research Trends. *Renew. Sustain. Energy Rev.* **2018**, *91*, 987–1018. [CrossRef]
15. Ambrosini, A.; Boubault, A.; Ho, C.K.; Banh, L.; Lewis, J.R. Influence of Application Parameters on Stability of Pyromark® 2500 Receiver Coatings. *AIP Conf. Proc.* **2019**, *2126*, 030002. [CrossRef]
16. Ho, C.K.; Mahoney, A.R.; Ambrosini, A.; Bencomo, M.; Hall, A.; Lambert, T.N. Characterization of Pyromark 2500 Paint for High-Temperature Solar Receivers. *J. Sol. Energy Eng.* **2014**, *136*, 014502. [CrossRef]
17. Bello, M.; Shanmugan, S. Achievements in Mid and High-Temperature Selective Absorber Coatings by Physical Vapor Deposition (PVD) for Solar Thermal Application-A Review. *J. Alloys Compd.* **2020**, *839*, 155510. [CrossRef]
18. Kennedy, C.E. *Review of Mid- to High-Temperature Solar Selective Absorber Materials*; National Renewable Energy Laboratory, Cole Boulevard: Golden, CO, USA, 2002.
19. Atkinson, C.; Sansom, C.L.; Almond, H.J.; Shaw, C.P. Coatings for Concentrating Solar Systems—A Review. *Renew. Sustain. Energy Rev.* **2015**, *45*, 113–122. [CrossRef]
20. Xu, K.; Du, M.; Hao, L.; Mi, J.; Yu, Q.; Li, S. A Review of High-Temperature Selective Absorbing Coatings for Solar Thermal Applications. *J. Mater.* **2020**, *6*, 167–182. [CrossRef]
21. Granqvist, C.G. Preparation of Thin Films and Nanostructured Coatings for Clean Tech Applications: A Primer. *Sol. Energy Mater. Sol. Cells* **2012**, *99*, 166–175. [CrossRef]
22. Price, H.; Lüpfer, E.; Kearney, D.; Zarza, E.; Cohen, G.; Gee, R.; Mahoney, R. Advances in Parabolic Trough Solar Power Technology. *J. Sol. Energy Eng.* **2002**, *124*, 109–125. [CrossRef]
23. Mwema, F.M.; Akinlabi, E.T.; Oladijo, O.P. Sustainability Issues in Sputtering Deposition Technology. In Proceedings of the International Conference on Industrial Engineering and Operations Management 2019, Toronto, ON, Canada, 23–25 October 2019; IEOM Society: Toronto, ON, Canada, 2019; pp. 737–744.
24. Ambrosini, A.; Lambert, T.N.; Bencomo, M.; Hall, A.; Van Every, K.; Siegel, N.P.; Ho, C.K. Improved High Temperature Solar Absorbers for Use in Concentrating Solar Power Central Receiver Applications. In Proceedings of the ASME 2011 5th International Conference on Energy Sustainability, Washington, DC, USA, 7–10 August 2011; pp. 587–594. [CrossRef]
25. Hall, A.; Ambrosini, A.; Ho, C. Solar Selective Coatings for Concentrating. *Adv. Mater. Process.* **2012**, *170*, 28–32.
26. Wang, X.; Ouyang, T.; Duan, X.; Ke, C.; Zhang, X.; Min, J.; Li, A.; Guo, W.; Cheng, X. Improved Solar Absorptance of WC/Co Solar Selective Absorbing Coating with Multimodal WC Particles. *Metals* **2017**, *7*, 137. [CrossRef]
27. Toru, D.; Quet, A.; De Sousa Meneses, D.; Del Campo, L.; Echegut, P. Influence of Microstructure and Composition on Optical Properties of Plasma Sprayed Al/Al₂O₃ Cermets. *J. Phys. Chem. C* **2015**, *119*, 5426–5433. [CrossRef]
28. Del Campo, L.; De Sousa Meneses, D.; Wittmann-Ténèze, K.; Bacciochini, A.; Denoirjean, A.; Echegut, P. Effect of Porosity on the Infrared Radiative Properties of Plasma-Sprayed Ytria-Stabilized Zirconia Ceramic Thermal Barrier Coatings. *J. Phys. Chem. C* **2014**, *118*, 13590–13597. [CrossRef]
29. Tului, M.; Arezzo, F.; Pawlowski, L. Optical Properties of Plasma Sprayed ZnO+Al₂O₃ Coatings. *Surf. Coat. Technol.* **2004**, *179*, 47–55. [CrossRef]
30. Singh, C.C.; Panda, E. Zinc Interstitial Threshold in Al-Doped ZnO Film: Effect on Microstructure and Optoelectronic Properties. *J. Appl. Phys.* **2018**, *123*, 165106. [CrossRef]
31. Tominaga, K.; Umez, N.; Mori, I.; Ushiro, T.; Moriga, T.; Nakabayashi, I. Properties of ZnO: In Film Prepared by Sputtering of Facing ZnO:In and Zn Targets. *J. Vac. Sci. Technol. A Vac. Surf. Film.* **1998**, *16*, 1213–1217. [CrossRef]
32. Pawlowski, L. *The Science and Engineering of Thermal Spray Coatings*; John Wiley & Sons: Chichester, UK, 2008; ISBN 9780470754085.
33. Hall, A.; Ambrosini, A.; Ho, C.; McCloskey, J.; Van Every, K.; Urrea, D.; Lambert, T.; Bencomo, M.; Mahoney, A.; Siegel, N. Solar Selective Coatings for Concentrating Solar Power Central Receivers. *Adv. Mater. Process.* **2011**, *28*, 28–32.
34. Ambrosini, A.; Lambert, T.N.; Boubault, A.; Hunt, A.; Davis, D.J.; Adams, D.; Hall, A.C. Thermal Stability of Oxide-Based Solar Selective Coatings for CSP Central Receivers. In Proceedings of the ASME 2015 9th International Conference on Energy Sustainability Collocated with the ASME 2015 Power Conference, the ASME 2015 13th International Conference on Fuel Cell Science, Engineering and Technology, and the ASME 2015 Nuclear Forum, San Diego, CA, USA, 28 June–2 July 2015; Volume 1, pp. 1–10. [CrossRef]
35. Ke, C.; Zhang, X.; Guo, W.; Li, Y.; Gong, D.Q.; Cheng, X. Solar Selective Coatings with Multilayered Structure Based on Thermal Spraying WC-Co Solar Absorption Layer. *Vacuum* **2018**, *152*, 114–122. [CrossRef]

36. Brousse-Pereira, E.; Wittmann-Teneze, K.; Bianchi, V.; Longuet, J.L.; Del Campo, L. Optical and Electrical Properties of Heterogeneous Coatings Produced by Aluminum Powder and Boehmite Suspension Plasma Spraying. *J. Therm. Spray Technol.* **2012**, *21*, 1110–1119. [\[CrossRef\]](#)
37. Zhu, J.; Gao, L.; Ma, Z.; Liu, Y.; Wang, F. Optical Property of $\text{La}_{1-x}\text{Sr}_x\text{TiO}_{3+\delta}$ Coatings Deposited by Plasma Spraying Technique. *Appl. Surf. Sci.* **2015**, *356*, 935–940. [\[CrossRef\]](#)
38. Deng, X.-Q.; Xue, M.-M.; Lv, Y.-L.; Li, R.-H.; Tong, J.-M.; Shi, G.-H.; Yang, Y.; Dong, Y.-C. Study on Spectral Selective Absorbing Coatings with Spinel Structures Fabricated via Plasma Spraying. *Vacuum* **2020**, *174*, 109214. [\[CrossRef\]](#)
39. Bunmephiphit, C.; Suriwong, T.; Jiajitsawat, S.; Dejang, N. Characterization of Ni-Al Solar Absorber Prepared by Flame Spray Technique. *Key Eng. Mater.* **2016**, *675–676*, 477–481. [\[CrossRef\]](#)
40. Wu, S.; Cheng, C.H.; Hsiao, Y.J.; Juang, R.C.; Wen, W.F. Fe_2O_3 Films on Stainless Steel for Solar Absorbers. *Renew. Sustain. Energy Rev.* **2016**, *58*, 574–580. [\[CrossRef\]](#)
41. Tulchinsky, D.; Uvarov, V.; Popov, I.; Mandler, D.; Magdassi, S. A Novel Non-Selective Coating Material for Solar Thermal Potential Application Formed by Reaction between Sol-Gel Titania and Copper Manganese Spinel. *Sol. Energy Mater. Sol. Cells* **2014**, *120*, 23–29. [\[CrossRef\]](#)
42. Carlsson, B.; Möller, K.; Köhl, M.; Frei, U.; Brunold, S. Qualification Test Procedure for Solar Absorber Surface Durability. *Sol. Energy Mater. Sol. Cells* **2000**, *61*, 255–275. [\[CrossRef\]](#)
43. Duan, X.; Zhang, X.; Ke, C.; Jiang, S.; Wang, X.; Li, S.; Guo, W.; Cheng, X. Microstructure and Optical Properties of Co-WC- Al_2O_3 Duplex Ceramic Metal-Dielectric Solar Selective Absorbing Coating Prepared by High Velocity Oxy-Fuel Spraying and Sol-Gel Method. *Vacuum* **2017**, *145*, 209–216. [\[CrossRef\]](#)
44. Barshilia, H.C.; Kumar, P.; Rajam, K.S.; Biswas, A. Structure and Optical Properties of Ag- Al_2O_3 Nanocermet Solar Selective Coatings Prepared Using Unbalanced Magnetron Sputtering. *Sol. Energy Mater. Sol. Cells* **2011**, *95*, 1707–1715. [\[CrossRef\]](#)
45. Gao, X.-H.; Guo, Z.-M.; Geng, Q.-F.; Ma, P.-J.; Wang, A.-Q.; Liu, G. Structure, Optical Properties and Thermal Stability of SS/TiC-ZrC/ Al_2O_3 Spectrally Selective Solar Absorber. *RSC Adv.* **2016**, *6*, 63867–63873. [\[CrossRef\]](#)
46. Gao, Y.; Xiong, J.; Gong, D.; Li, J.; Ding, M. Improvement of Solar Absorbing Property of Ni-Mo Based Thermal Spray Coatings by Laser Surface Treatment. *Vacuum* **2015**, *121*, 64–69. [\[CrossRef\]](#)
47. Shah, A.A.; Gupta, M.C. Spectral Selective Surfaces for Concentrated Solar Power Receivers by Laser Sintering of Tungsten Micro and Nano Particles. *Sol. Energy Mater. Sol. Cells* **2013**, *117*, 489–493. [\[CrossRef\]](#)
48. Sevillano, F.; Poza, P.; Múnez, C.J.; Vezzù, S.; Rech, S.; Trentin, A. Cold-Sprayed Ni- Al_2O_3 Coatings for Applications in Power Generation Industry. *J. Therm. Spray Technol.* **2013**, *22*, 772–782. [\[CrossRef\]](#)
49. Shah, A.A.; Ungaro, C.; Gupta, M.C. High Temperature Spectral Selective Coatings for Solar Thermal Systems by Laser Sintering. *Sol. Energy Mater. Sol. Cells* **2015**, *134*, 209–214. [\[CrossRef\]](#)
50. Pang, X.; Wei, Q.; Zhou, J.; Ma, H. High-Temperature Tolerance in Multi-Scale Cermet Solar-Selective Absorbing Coatings Prepared by Laser Cladding. *Materials* **2018**, *11*, 1037. [\[CrossRef\]](#)
51. Ungaro, C.; Gray, S.K.; Gupta, M.C. Black Tungsten for Solar Power Generation. *Appl. Phys. Lett.* **2013**, *103*, 071105. [\[CrossRef\]](#)
52. Ghmari, F.; Ghbara, T.; Laroche, M.; Carminati, R.; Greffet, J.-J. Influence of Microroughness on Emissivity. *J. Appl. Phys.* **2004**, *96*, 2656–2664. [\[CrossRef\]](#)
53. Sai, H.; Yugami, H.; Kanamori, Y.; Hane, K. Solar Selective Absorbers Based on Two-Dimensional W Surface Gratings with Submicron Periods for High-Temperature Photothermal Conversion. *Sol. Energy Mater. Sol. Cells* **2003**, *79*, 35–49. [\[CrossRef\]](#)
54. Rico, A.; Salazar, A.; Escobar, M.E.; Rodriguez, J.; Poza, P. Optimization of Atmospheric Low-Power Plasma Spraying Process Parameters of Al_2O_3 -50wt% Cr_2O_3 Coatings. *Surf. Coat. Technol.* **2018**, *354*, 281–296. [\[CrossRef\]](#)
55. Astarita, A.; Genna, S.; Leone, C.; Minutolo, F.M.C.; Rubino, F.; Squillace, A. Study of the Laser Remelting of a Cold Sprayed Titanium Layer. *Procedia CIRP* **2015**, *33*, 452–457. [\[CrossRef\]](#)
56. Rubino, F.; Paradiso, V.; Astarita, A.; Carlone, P.; Squillace, A. Advances in Titanium on Aluminium Alloys Cold Spray Coatings. In *Cold-Spray Coatings*; Springer International Publishing: Cham, Switzerland, 2018; pp. 225–249.
57. Rubino, F.; Astarita, A.; Carlone, P. Thermo-Mechanical Finite Element Modeling of the Laser Treatment of Titanium Cold-Sprayed Coatings. *Coatings* **2018**, *8*, 219. [\[CrossRef\]](#)
58. Viscusi, A.; Astarita, A.; Gatta, R.D.; Rubino, F. A Perspective Review on the Bonding Mechanisms in Cold Gas Dynamic Spray. *Surf. Eng.* **2019**, *35*, 743–771. [\[CrossRef\]](#)
59. Paradiso, V.; Rubino, F.; Tucci, F.; Astarita, A.; Carlone, P. Thermo-Mechanical Modeling of Laser Treatment on Titanium Cold-Spray Coatings. *AIP Conf. Proc.* **2018**, *1960*, 100011. [\[CrossRef\]](#)
60. Rubino, F.; Astarita, A.; Carlone, P.; Genna, S.; Leone, C.; Memola Capece Minutolo, F.; Squillace, A. Selective Laser Post-Treatment on Titanium Cold Spray Coatings. *Mater. Manuf. Process.* **2016**, *31*, 1500–1506. [\[CrossRef\]](#)
61. Carlone, P.; Astarita, A.; Rubino, F.; Pasquino, N.; Aprea, P. Selective Laser Treatment on Cold-Sprayed Titanium Coatings: Numerical Modeling and Experimental Analysis. *Metall. Mater. Trans. B* **2016**, *47*, 3310–3317. [\[CrossRef\]](#)
62. Rubino, F.; Ammendola, P.; Astarita, A.; Raganati, F.; Squillace, A.; Viscusi, A.; Chirone, R.; Carrino, L. An Innovative Method to Produce Metal Foam Using Cold Gas Dynamic Spray Process Assisted by Fluidized Bed Mixing of Precursors. *Key Eng. Mater.* **2015**, *651–653*, 913–918. [\[CrossRef\]](#)
63. Kuravi, S.; Trahan, J.; Goswami, D.Y.; Rahman, M.M.; Stefanakos, E.K. Thermal Energy Storage Technologies and Systems for Concentrating Solar Power Plants. *Prog. Energy Combust. Sci.* **2013**, *39*, 285–319. [\[CrossRef\]](#)

64. González-Roubaud, E.; Pérez-Osorio, D.; Prieto, C. Review of Commercial Thermal Energy Storage in Concentrated Solar Power Plants: Steam vs. Molten Salts. *Renew. Sustain. Energy Rev.* **2017**, *80*, 133–148. [\[CrossRef\]](#)
65. Gil, A.; Medrano, M.; Martorell, I.; Lázaro, A.; Dolado, P.; Zalba, B.; Cabeza, L.F. State of the Art on High Temperature Thermal Energy Storage for Power Generation. Part 1—Concepts, Materials and Modellization. *Renew. Sustain. Energy Rev.* **2010**, *14*, 31–55. [\[CrossRef\]](#)
66. Walczak, M.; Pineda, F.; Fernández, Á.G.; Mata-Torres, C.; Escobar, R.A. Materials Corrosion for Thermal Energy Storage Systems in Concentrated Solar Power Plants. *Renew. Sustain. Energy Rev.* **2018**, *86*, 22–44. [\[CrossRef\]](#)
67. Olivares, R.I. The Thermal Stability of Molten Nitrite/Nitrates Salt for Solar Thermal Energy Storage in Different Atmospheres. *Sol. Energy* **2012**, *86*, 2576–2583. [\[CrossRef\]](#)
68. Sarvghad, M.; Delkasar Maher, S.; Collard, D.; Tassan, M.; Will, G.; Steinberg, T.A. Materials Compatibility for the next Generation of Concentrated Solar Power Plants. *Energy Storage Mater.* **2018**, *14*, 179–198. [\[CrossRef\]](#)
69. Bell, S.; Steinberg, T.; Will, G. Corrosion Mechanisms in Molten Salt Thermal Energy Storage for Concentrating Solar Power. *Renew. Sustain. Energy Rev.* **2019**, *114*, 109328. [\[CrossRef\]](#)
70. Medrano, M.; Gil, A.; Martorell, I.; Potau, X.; Cabeza, L.F. State of the Art on High-Temperature Thermal Energy Storage for Power Generation. Part 2—Case Studies. *Renew. Sustain. Energy Rev.* **2010**, *14*, 56–72. [\[CrossRef\]](#)
71. Vignarooban, K.; Xu, X.; Arvay, A.; Hsu, K.; Kannan, A.M. Heat Transfer Fluids for Concentrating Solar Power Systems—A Review. *Appl. Energy* **2015**, *146*, 383–396. [\[CrossRef\]](#)
72. Ibrahim, A.; Peng, H.; Riaz, A.; Abdul Basit, M.; Rashid, U.; Basit, A. Molten Salts in the Light of Corrosion Mitigation Strategies and Embedded with Nanoparticles to Enhance the Thermophysical Properties for CSP Plants. *Sol. Energy Mater. Sol. Cells* **2021**, *219*, 110768. [\[CrossRef\]](#)
73. Groll, M.; Brost, O.; Heine, D. Corrosion of Steels in Contact with Salt Eutectics as Latent Heat Storage Materials: Influence of Water and Other Impurities. *Heat Recover. Syst. CHP* **1990**, *10*, 567–572. [\[CrossRef\]](#)
74. Cuevas-Arteaga, C.; Uruchurtu-Chavarín, J.; Porcayo-Calderon, J.; Izquierdo-Montalvo, G.; Gonzalez, J. Study of Molten Salt Corrosion of HK-40 m Alloy Applying Linear Polarization Resistance and Conventional Weight Loss Techniques. *Corros. Sci.* **2004**, *46*, 2663–2679. [\[CrossRef\]](#)
75. Tian, Y.; Zhao, C.Y. A Review of Solar Collectors and Thermal Energy Storage in Solar Thermal Applications. *Appl. Energy* **2013**, *104*, 538–553. [\[CrossRef\]](#)
76. Vignarooban, K.; Pugazhendhi, P.; Tucker, C.; Gervasio, D.; Kannan, A.M. Corrosion Resistance of Hastelloys in Molten Metal-Chloride Heat-Transfer Fluids for Concentrating Solar Power Applications. *Sol. Energy* **2014**, *103*, 62–69. [\[CrossRef\]](#)
77. Steinmann, W.-D. Thermal energy storage systems for concentrating solar power (CSP) plants. In *Concentrating Solar Power Technology*; Lovegrove, K., Stein, W., Eds.; Woodhead Publishing, Elsevier: Amsterdam, The Netherlands, 2012; pp. 362–394.
78. Tortorelli, P.F.; Bishop, P.S.; DiStefano, J.R. *Selection of Corrosion-Resistant Materials for Use in Molten Nitrate Salts*; Oak Ridge National Lab.: Oak Ridge, TN, USA, 1989. [\[CrossRef\]](#)
79. Tortorelli, P.F.; Bishop, P.S. *Influence of Compositional Modifications on the Corrosion of Iron Aluminides of Molten Nitrate Salts*; Oak Ridge National Lab.: Oak Ridge, TN, USA, 1991. [\[CrossRef\]](#)
80. Gonzalez, M.; Nithiyanantham, U.; Carbó-Argibay, E.; Bondarchuk, O.; Grosu, Y.; Faik, A. Graphitization as Efficient Inhibitor of the Carbon Steel Corrosion by Molten Binary Nitrate Salt for Thermal Energy Storage at Concentrated Solar Power. *Sol. Energy Mater. Sol. Cells* **2019**, *203*, 110172. [\[CrossRef\]](#)
81. Ding, W.; Bonk, A.; Bauer, T. Molten Chloride Salts for next Generation CSP Plants: Selection of Promising Chloride Salts & Study on Corrosion of Alloys in Molten Chloride Salts. *AIP Conf. Proc.* **2019**, *2126*, 200014. [\[CrossRef\]](#)
82. Dariva, C.G.; Galio, A.F. Corrosion Inhibitors—Principles, Mechanisms and Applications. In *Developments in Corrosion Protection*; Aliofkhazraei, M., Ed.; InTech: London, UK, 2014.
83. Ding, W.; Bonk, A.; Gussone, J.; Bauer, T. Electrochemical Measurement of Corrosive Impurities in Molten Chlorides for Thermal Energy Storage. *J. Energy Storage* **2018**, *15*, 408–414. [\[CrossRef\]](#)
84. Ding, W.; Bonk, A.; Gussone, J.; Bauer, T. Cyclic Voltammetry for Monitoring Corrosive Impurities in Molten Chlorides for Thermal Energy Storage. *Energy Procedia* **2017**, *135*, 82–91. [\[CrossRef\]](#)
85. Singh, H.; Puri, D.; Prakash, S.; Ghosh, T.K. Hot Corrosion of a Plasma Sprayed Ni₃Al Coating on a Ni-Base Superalloy. *Mater. Corros.* **2007**, *58*, 857–866. [\[CrossRef\]](#)
86. Gomez-Vidal, J.C.; Morton, E. Castable Cements to Prevent Corrosion of Metals in Molten Salts. *Sol. Energy Mater. Sol. Cells* **2016**, *153*, 44–51. [\[CrossRef\]](#)
87. Gomez-Vidal, J.C.; Fernandez, A.G.; Tirawat, R.; Turchi, C.; Huddleston, W. Corrosion Resistance of Alumina-Forming Alloys against Molten Chlorides for Energy Production. I: Pre-Oxidation Treatment and Isothermal Corrosion Tests. *Sol. Energy Mater. Sol. Cells* **2017**, *166*, 222–233. [\[CrossRef\]](#)
88. Gomez-Vidal, J.C.; Fernandez, A.G.; Tirawat, R.; Turchi, C.; Huddleston, W. Corrosion Resistance of Alumina Forming Alloys against Molten Chlorides for Energy Production. II: Electrochemical Impedance Spectroscopy under Thermal Cycling Conditions. *Sol. Energy Mater. Sol. Cells* **2017**, *166*, 234–245. [\[CrossRef\]](#)
89. Agüero, A.; García de Blas, F.J.; García, M.C.; Muelas, R.; Román, A. Thermal Spray Coatings for Molten Carbonate Fuel Cells Separator Plates. *Surf. Coat. Technol.* **2001**, *146–147*, 578–585. [\[CrossRef\]](#)

90. Trisancho-Reyes, J.L.; Chacón-Nava, J.G.; Peña-Ballesteros, D.Y.; Gaona-Tiburcio, C.; Gonzalez-Rodriguez, J.G.; Martínez-Villafañe, A.; Almeraya-Calderón, F. Hot Corrosion Behaviour of NiCrFeNbMoTiAl Coating in Molten Salts at 700 °C by Electrochemical Techniques. *Int. J. Electrochem. Sci.* **2011**, *6*, 432–441.
91. Agüero, A. Progress in the Development of Coatings for Protection of New Generation Steam Plant Components. *Energy Mater.* **2008**, *3*, 35–44. [\[CrossRef\]](#)
92. Ou, X.; Sun, Z.; Sun, M.; Zou, D. Hot-Corrosion Mechanism of Ni-Cr Coatings at 650 °C under Different Simulated Corrosion Conditions. *J. China Univ. Min. Technol.* **2008**, *18*, 444–448. [\[CrossRef\]](#)
93. Jiang, S.M.; Xu, C.Z.; Li, H.Q.; Ma, J.; Gong, J.; Sun, C. High Temperature Corrosion Behaviour of a Gradient NiCoCrAlYSi Coating I: Microstructure Evolution. *Corros. Sci.* **2010**, *52*, 1746–1752. [\[CrossRef\]](#)
94. Li, T.; Zhou, Y.; Li, M.; Li, Z. High Temperature Corrosion Behavior of a Multilayer CrAlN Coating Prepared by Magnetron Sputtering Method on a K38G Alloy. *Surf. Coat. Technol.* **2008**, *202*, 1985–1993. [\[CrossRef\]](#)
95. Ren, X.; Wang, F.; Wang, X. High-Temperature Oxidation and Hot Corrosion Behaviors of the NiCr–CrAl Coating on a Nickel-Based Superalloy. *Surf. Coat. Technol.* **2005**, *198*, 425–431. [\[CrossRef\]](#)
96. Lauwerens, W.; De Boeck, A.; Thijs, M.; Claessens, S.; Van Stappen, M.; Steenackers, P. PVD Al–Ti and Al–Mn Coatings for High Temperature Corrosion Protection of Sheet Steel. *Surf. Coat. Technol.* **2001**, *146–147*, 27–32. [\[CrossRef\]](#)
97. Senderowski, C.; Cinca, N.; Dosta, S.; Cano, I.G.; Guilemany, J.M. The Effect of Hot Treatment on Composition and Microstructure of HVOF Iron Aluminide Coatings in Na₂SO₄ Molten Salts. *J. Therm. Spray Technol.* **2019**, *28*, 1492–1510. [\[CrossRef\]](#)
98. Audigié, P.; Encinas-Sánchez, V.; Juez-Lorenzo, M.; Rodríguez, S.; Gutiérrez, M.; Pérez, F.J.; Agüero, A. High Temperature Molten Salt Corrosion Behavior of Aluminide and Nickel-Aluminide Coatings for Heat Storage in Concentrated Solar Power Plants. *Surf. Coat. Technol.* **2018**, *349*, 1148–1157. [\[CrossRef\]](#)
99. Audigié, P.; Encinas-Sánchez, V.; Rodríguez, S.; Pérez, F.J.; Agüero, A. High Temperature Corrosion beneath Carbonate Melts of Aluminide Coatings for CSP Application. *Sol. Energy Mater. Sol. Cells* **2020**, *210*, 110514. [\[CrossRef\]](#)
100. Grégoire, B.; Oskay, C.; Meißner, T.M.; Galetz, M.C. Corrosion Performance of Slurry Aluminide Coatings in Molten NaCl–KCl. *Sol. Energy Mater. Sol. Cells* **2021**, *223*. [\[CrossRef\]](#)
101. Vignarooban, K.; Xu, X.; Wang, K.; Molina, E.E.; Li, P.; Gervasio, D.; Kannan, A.M. Vapor Pressure and Corrosivity of Ternary Metal-Chloride Molten-Salt Based Heat Transfer Fluids for Use in Concentrating Solar Power Systems. *Appl. Energy* **2015**, *159*, 206–213. [\[CrossRef\]](#)
102. McConohy, G.; Kruizenga, A. Molten Nitrate Salts at 600 and 680 °C: Thermophysical Property Changes and Corrosion of High-Temperature Nickel Alloys. *Sol. Energy* **2014**, *103*, 242–252. [\[CrossRef\]](#)
103. Liu, B.; Wei, X.; Wang, W.; Lu, J.; Ding, J. Corrosion Behavior of Ni-Based Alloys in Molten NaCl–CaCl₂–MgCl₂ Eutectic Salt for Concentrating Solar Power. *Sol. Energy Mater. Sol. Cells* **2017**, *170*, 77–86. [\[CrossRef\]](#)
104. Shankar, A.R.; Kanagasundar, A.; Mudali, U.K. Corrosion of Nickel-Containing Alloys in Molten LiCl–KCl Medium. *Corrosion* **2013**, *69*, 48–57. [\[CrossRef\]](#)
105. Trisancho-Reyes, J.L.; Almeraya-Calderón, F.; Chacón-Nava, J.G. Hot Corrosion on NiCrFeNbMoTiAl Coating, Plasma Spray Deposited. *Sci. Tech. Año XVI* **2010**, *1*, 379–383. [\[CrossRef\]](#)
106. Porcayo-Calderon, J.; Sotelo-Mazon, O.; Salinas-Bravo, V.M.; Arrieta-Gonzalez, C.D.; Ramos-Hernandez, J.J.; Cuevas-Arteaga, C. Electrochemical Performance of Ni₂₀Cr Coatings Applied by Combustion Powder Spray in ZnCl₂–KCl Molten Salts. *Int. J. Electrochem. Sci.* **2012**, *7*, 1134–1148.
107. Porcayo-Calderón, J.; Sotelo-Mazón, O.; Casales-Díaz, M.; Ascencio-Gutiérrez, J.A.; Salinas-Bravo, V.M.; Martínez-Gómez, L. Electrochemical Study of Ni₂₀Cr Coatings Applied by HVOF Process in ZnCl₂–KCl at High Temperatures. *J. Anal. Methods Chem.* **2014**, *2014*, 503618. [\[CrossRef\]](#)
108. Mohanty, B.P.; Shores, D.A. Role of Chlorides in Hot Corrosion of a Cast Fe–Cr–Ni Alloy. Part I: Experimental Studies. *Corros. Sci.* **2004**, *46*, 2893–2907. [\[CrossRef\]](#)
109. Shores, D.A.; Mohanty, B.P. Role of Chlorides in Hot Corrosion of a Cast Fe–Cr–Ni Alloy. Part II: Thermochemical Model Studies. *Corros. Sci.* **2004**, *46*, 2909–2924. [\[CrossRef\]](#)
110. Ishitsuka, T.; Nose, K. Stability of Protective Oxide Films in Waste Incineration Environment—Solubility Measurement of Oxides in Molten Chlorides. *Corros. Sci.* **2002**, *44*, 247–263. [\[CrossRef\]](#)
111. Marulanda A., J. L. Corrosión En Sales Fundidas de Un Acero Recubierto Mediante Rociado Térmico Por Llama. *Prospectiva* **2014**, *12*, 1. [\[CrossRef\]](#)
112. Gomez-Vidal, J.C. Corrosion Resistance of MCrAlX Coatings in a Molten Chloride for Thermal Storage in Concentrating Solar Power Applications. *Npj Mater. Degrad.* **2017**, *1*, 1–8. [\[CrossRef\]](#)
113. Gomez-Vidal, J.C.; Noel, J.; Weber, J. Corrosion Evaluation of Alloys and MCrAlX Coatings in Molten Carbonates for Thermal Solar Applications. *Sol. Energy Mater. Sol. Cells* **2016**, *157*, 517–525. [\[CrossRef\]](#)
114. Meier, G.H.; Pettit, F.S. High-Temperature Corrosion of Alumina-Forming Coatings for Superalloys. *Surf. Coat. Technol.* **1989**, *39–40*, 1–17. [\[CrossRef\]](#)
115. Jiang, S.M.; Peng, X.; Bao, Z.B.; Liu, S.C.; Wang, Q.M.; Gong, J.; Sun, C. Preparation and Hot Corrosion Behaviour of a MCrAlY + AlSiY Composite Coating. *Corros. Sci.* **2008**, *50*, 3213–3220. [\[CrossRef\]](#)
116. Zhang, T.; Huang, C.; Lan, H.; Du, L.; Zhang, W. Oxidation and Hot Corrosion Behavior of Plasma-Sprayed MCrAlY–Cr₂O₃ Coatings. *J. Therm. Spray Technol.* **2016**, *25*, 1208–1216. [\[CrossRef\]](#)

-
117. Raiman, S.S.; Mayes, R.T.; Kurley, J.M.; Parrish, R.; Vogli, E. Amorphous and Partially-Amorphous Metal Coatings for Corrosion Resistance in Molten Chloride Salt. *Sol. Energy Mater. Sol. Cells* **2019**, *201*, 110028. [[CrossRef](#)]
 118. Ma, H.R.; Li, J.W.; Chang, C.T.; Wang, X.M.; Li, R.W. Passivation Behavior of Fe-Based Amorphous Coatings Prepared by High-Velocity Air/Oxygen Fuel Processes. *J. Therm. Spray Technol.* **2017**, *26*, 2040–2047. [[CrossRef](#)]
 119. US Department of Energy's Solar Energy Technologies Office the SunShot Initiative. Available online: <https://www.energy.gov/eere/solar/sunshot-initiative> (accessed on 1 May 2021).
 120. European Commission The Strategic Energy Technology (SET) Plan. Available online: <https://op.europa.eu/en/publication-detail/-/publication/064a025d-0703-11e8-b8f5-01aa75ed71a1> (accessed on 1 May 2021).